ORIGINAL ARTICLE

Effect of Optogenetic Stimulation Parameters on Firing Rate of Basal Ganglia Neurons in Parkinsonian State BG and RT Networks

Nazlar Ghasemzadeh [1], Fereidoun Nowshiravan Rahatabad [1 *], Siamak Haghipour [2], Shabnam Andalibi Miandoab [3, 4*], Keivan Maghooli [1]

[1] *Department of Biomedical Engineering, Science and Research Branch, Islamic Azad university, Tehran, Iran*

[2] *Department of Biomedical Engineering, Tabriz Branch, Islamic Azad university, Tabriz, Iran*

[3] *Department of Electrical Engineering, Tabriz Branch, Islamic Azad university, Tabriz, Iran*

[4] *Biophotonic Research Center, Tabriz Branch, Islamic Azad University, Tabriz, Iran*

*Corresponding Authors: Fereidoun Nowshiravan Rahatabad, Shabnam Andalibi Miandoab
Email: nowshiravan@srbiau.ac.ir, sh.andalibi@iaut.ac.ir

Received: 11 August 2023 / Accepted: 14 November 2023

Abstract

Purpose: Parkinson's disease is a neurodegenerative disorder that affects the basal ganglia of the brain, which plays an important role in movement. Basal Ganglia-Thalamic network model including Subthalamic nucleus, Globus Pallidus externa, Globus Pallidus interna and Thalamus neurons. Optogenetics is a combination of optical and genetic tools used to stimulate basal ganglia neurons by light-sensitive ion channels (opsins) to eliminate the pathological effects of Parkinson's disease.

Materials and Methods: To analyze the effect of optogenetic stimulation on Parkinsonian nervous systems, two complete models of BG and RT (including STN, GPe, Gpi, and TH neurons) have been selected and developed for Parkinson's disease and to apply three and four-state optogenetic stimulation. For this purpose, ChETA, ChRwt, and NpHR opsins have been selected in three-state and four-state stimulations and different stimulation conditions according to different parameters in both models have been investigated.

Results: To evaluate the performance of two models for each gene in three- and four-state stimulation conditions with different values of basic parameters, the value of error index is calculated and stimulation conditions that created an error index equal to zero have been introduced as optimal conditions. Based on the results, frequencies of 20 and 200 Hz in the four-state ChRwt model and frequency of 80 Hz in the three-state ChETA model have been introduced as optimal genes, frequencies, and models. To verify the developed model, the obtained results have been compared with the results of experimental studies.

Conclusion: In optimal conditions, STN provides excitatory input and GPe provide appropriate inhibitory input to GPi, and GPi can provide appropriate inhibitory input to TH, and as a result, its function improves and pathological effects of Parkinson's disease disappear. The response of GPe neurons is consistent with the experimental results and the response of other neurons is also similar to the response of GPe neurons.

Keywords: Parkinson's Disease; Optogenetic Stimulation; Basal Ganglia Network Model; Rubin-Terman Network Model.

DOI: https://doi.org/10.18502/fbt.v11i3.15883

1. Introduction

Parkinson's Disease (PD) is a neurodegenerative disease [1, 2] that created by the disruption of the Basal Ganglia (BG) in the Substantia nigra pars Compacta (SNC) and Ventral Tegmental Area (VTA) [3]. Basal Ganglia is the Subcortical structure of the brain which consists of the Subthalamic Nucleus (STN), Globus Pallidus interna (GPi), Globus Pallidus externa (GPe), and Thalamus (TH) that has an important role in the dynamic system [4]. Compared to electrical methods and drug treatment, optogenetic light stimulation methods are suitable tools in neuroscience studies due to their higher speed and precision and less damage [5].

Parkinson's disease destroys the dopamine-producing neurons and degenerates them that causes to disrupt the ion channels and their concentration. In the electrophysiology methods, special metal electrodes and electric current have been used to stimulate the nervous systems and restore the function of dopamine-producing neurons. In optical stimulation of the nervous system considering that the nervous system itself, specially is not sensitive to light, this process is done by stimulation of protein channels sensitive to light (opsins) in a way that, these protein channels in nerve cells are generated by genetic methods and stimulated by light delivery. To send stimulating light to different parts of the brain's nervous system, it is necessary to design and manufacture different optical probes to stimulate the nervous system. Light delivery technology and optical sources used to light delivery to activation of defined opsins and the change in the biological function of cells is one of the most important parts of the light physics of this process [6-10]. Optical current caused by an optical pulse in light depends on different factors such as the opsin properties used, the wavelength of the light, the intensity, and duration of the radiation [11, 12]. In general, the important characteristics of radiation light sources used in optogenetics are properties of wavelength required to control the opsin used, temporal control of light radiation, whether the light should be focused or wide, should be multi-beam or single beam, providing a diode light source necessary or not and how light spreads in biological tissue [13-15]. So, optogenetic stimulation is the combination of genetic and optical tools for the treatment of Parkinson's disease with the stimulation of special neurons [16, 17], which was first used by Deisseroth *et al.* (2006) to precisely control the human brain [18]. Optogenetics refers to a technique in which neuronal activity by opsins, light-sensitive ion channels, can be applied to the desired neuronal population, resulting in depolarization (activation) and hyperpolarization (inactivation) of the neuronal membrane. There are different types of activating and inhibitory opsins. Such as Channelrhodopsin-2 (ChR2) E123T mutation; creates faster kinetics but reduces photocurrent amplitude (ChETA) ،ChR1-VChR1 chimera with E122T and E162T mutations (C1V1) ،Red-activatable Channelrhodopsin (ReachR) that are activating opsins and Halorhodopsin (NpHR), Light-activated outward proton pump from Halorubrum sodomense (Aarch) and Light-activated outward proton pump from Leptosphaeria (Mac) are inhibitory opsins. The most common activating opsin is ChR2, which is a necessary tool in neuroscience that causes neural depolarization. NpHR is the first photogenetic tool that effectively inhibits nerve activity [19-27].

The studies that have been carried out in this field up to now have tried to provide a suitable model for simulating neurons of the basal ganglia of the brain, which are the target neurons in Parkinson's disease. Since, the application of optogenetic stimulation in clinical conditions brings life risks and a lot of time and financial losses, it is very important to provide a suitable model beside clinical studies that is closest to the experimental conditions and includes all the conditions and influential parts. So by having such a model, it is possible to predict the parameters and suitable stimulation conditions to have the best effect with the least damage. Moreover, the response of the neurons resulting from the model has been discussed as firing patterns, applying different electrical and optical stimulations have been investigated and protein channels have been selected. Rosa *et al.* (2012) [28], in a computational model, have investigated the function of TH cells in the nervous system of BG for PD by applying Deep Brain Stimulation (DBS) by electrical stimulation method.

Stefanescu *et al.* (2013) [27] have represented the computational models of optical stimulations (optogenetic) of the opsins as three-state and four-state stimulation, and for this purpose, they have selected protein channels of ChR2 (ChETA,ChRwt) and have considered neural response as firing patterns. Shivakeshuvan Ratnadurai-Giridhaan *et al.* (2017) [29], in an initial computational model, consisting of just STN and GPe, have compared the effects of DBS stimulation and optogenetic on STN-GPe nervous system in PD by the

selection of ChR2 and NpHR protein channels. Honghui Zhang *et al.* (2020) [19], by presenting a basic computational model, investigated the function of the STN-GPe nervous system in Parkinson's disease by applying optogenetic stimulation and selected ChR2 and NpHR protein channels. Ghasemzadeh *et al.* (2023) [30] have considered the basal ganglia network of the brain (STN, GPe, GPi, TH) and have examined the effect of optogenetic stimulation by NpHR and ChR2 opsins as well as monophasic and biphasic electrical stimulation on the BG network model Parkinsonian conditions.

In this article, to achieve good results, we have tried to consider a computational modeling method, including all the effective parts of the neurons of the basal ganglia of the pathological effects of Parkinson's disease. So that by applying optogenetic stimulation in different conditions and simulating the desired model, we can investigate the effect on the response of different neurons and control Parkinson's disease in the best way. To achieve this goal, it has been tried to consider two complete Basal Ganglia-thalamic (BG) and Rubin-Terman (RT) models for simulating neurons of the basal ganglia nervous system, so that it includes all parts affected neurons, including TH, GPi, Gpe, and STN neurons with different connections, so that the study results are closest to experimental and clinical studies and the effect of different parts can be evaluated. In both models, different opsins ChR2 (ChETA, ChRwt) and NpHR were considered in the analysis of the effects of three-state and four-state optogenetic stimulations in Parkinson's disease and we have studied the response of all neurons of both BG and RT network models to various optogenetic stimulation. The basic parameters affecting the results include frequency (f), number of pulses (ns), pulse width (ton), and light stimulation intensity (A).

In this paper, by presenting a complete model, a model that can include all parts and neurons of the basal ganglia of the brain affected by Parkinson's disease, has been considered and also the effect of optogenetic stimulation on it has been analyzed. Our main goal in this paper is to investigate and compare the responses of BG and RT network model neurons (TH, STN, Gpe, and GPi) with the responses of neurons in experimental studies. Since, to record the neuronal responses, it is necessary to place deep electrodes in the deep areas of the brain and the Local Field Potential (LFP) of these neurons should be extracted, so, it is difficult to perform this type of experiment on humans and it is not possible to access this information through recorded EEG signals. To achieve the results very close to clinical conditions, the results obtained in this paper have been compared with the results of experimental studies. In these experimental studies [16, 25], the neuronal responses have been done in vitro (outside the body of the living organism) with the patch-clamp method of parvalbumin neurons related to the hippocampal part of the rat brain with virus injection during 2 to 3 weeks. Selected opsins are ChETA and ChRwt and the stimulation conditions are light intensity of 1.4 mw/mm^2, 470 nm blue light with a pulse width of 2 ms at a constant voltage of -60 mV in the frequency range of 10-200 Hz. In the following, by selecting the conditions that are closest to the experimental results, the effect of the basic parameters on the introduced models has been studied. The basic parameters that have been studied in the improvement of Parkinson's disease in this paper include the selection of appropriate opsin and effective stimulation conditions.

For this purpose, ChETA, ChRwt, and NpHR opsins have been investigated in three-state and four-state stimulation modes. Also, stimulation conditions including frequency (f), number of pulses (ns), pulse width (ton) and intensity of stimulation light (A) have been considered. Since opsins may experience reaction fatigue and lose their effectiveness with prolonged stimulation, and as a result, their performance deteriorates. Therefore, we continued to study both long and short stimulation in BG and RT models with different basic parameters for different opsins and introduced suitable conditions for each. In the end, to evaluate different stimulation conditions, the value of Error Index (EI) was calculated in the performance of each of the models, and in each of the modes, the conditions that have the minimum error index were introduced as optimal conditions. Determining the optimal conditions in the complete BG and RT network models by applying three- and four-state optogenetic stimulations by the selection of effective opsins of ChETA, ChRwt, and NpHR leads to achieving conditions in which the performance of the BG and RT network models have been improved and the pathological effects caused by PD disappear. In this way, in optimal conditions, STN neurons provide excitatory input and GPe neurons provide appropriate inhibitory input to GPi neurons, and GPi neurons are able to provide appropriate inhibitory input to TH neurons, as a result, its function improves and pathological effects of PD dissolves. Therefore, by obtaining optimal conditions for optogenetic stimulation, it is possible to obtain suitable

ranges for basic parameters such as frequency (f), number of stimulation pulses (ns), pulse width (ton), light stimulation intensity (A) and introduce the best conditions for the clinical applications of optogenetic stimulation in Parkinson's disease with the least damage to the brain tissue and provide the basis for the effective clinical application of optogenetic stimulation in all types of neurodegenerative diseases, especially Parkinson's.

2. Materials and Methods

2.1. Basal Ganglia-Thalamic Network and Rubin Terman Model

Since Parkinson's disease affects the basal ganglia of the brain, in this paper, a complete model including all the affected parts has been considered so that the study results are the closest to experimental and clinical studies and we can study the effect of the performance of each part separately. In this paper, the complete model of the computational network has been considered based on the computational network model of Terman *et al.* [28, 31, 32]. This model includes all the subdivisions affected by PD, including TH, GPi, GPe, and STN. In Figure 1(a, b), the BG and RT network models that include TH, GPi, Gpe, and STN neurons with sparse connections between TH, GPi, Gpe, and STN neurons have been shown. According to Figure 1a, thar is for the BG network model, STN applies excitatory input to GPi, and GPe applies inhibitory input to GPi. GPi also applies inhibitory input to TH. In Figure 1b, the RT network model has been represented in which each STN neuron stimulates three GPe neurons and one GPi neuron, each GPe neuron inhibits two STN neurons, two GPe neurons and two GPi neurons, and finally, each GPi neuron inhibits eight TH neurons. For both BG and RT networks, the SMC input has been considered as a series of monophasic current pulses with an amplitude of $3.5\ uA/cm^2 = 0.035pA/\mu m^2$ with a pulse width of 5ms. The I_appcurrent is applied as a constant and positive current to each of the GPi, GPe and STN neurons. Three and four-state optogenetic stimulations with effective opsins ChETA, ChRwt and NpHR are also applied to each STN, Gpe, and GPi neurons as suitable stimulation. In this way, by applying appropriate stimulation, the excitatory input from the STN neurons to the GPi neurons and the inhibitory input from the GPe neurons to the GPi neurons have been increased, and then the inhibitory input from the GPi neurons to the TH neurons also increases. As a result, GPi increases the ability to respond to SMC by exerting inhibitory input to TH, improves the function of TH neurons, and eliminates the pathological effects caused by Parkinson's disease. But if proper stimulation is not applied, errors in the function of TH neurons will be observed. This is despite the fact that in other references [22], the Iapp current was only applied to GPe neurons and the exact place for applying the appropriate stimulation in the model was not specified to which neurons the stimulation has been applied. BG and RT network model cells have been modeled as conductance-based differential equations based on the Hodgkin-Huxley model.

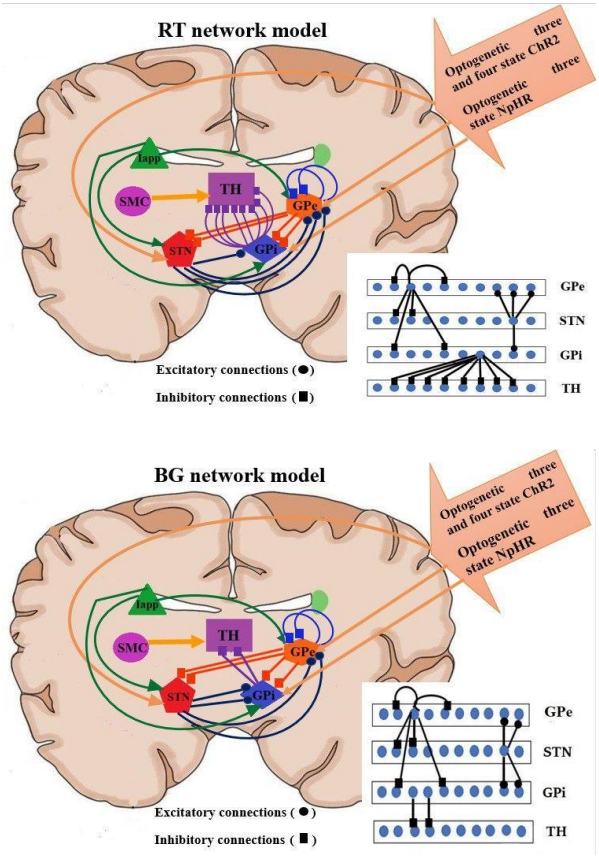

Figure 1. (a) BG network model including GPe, GPi, TH, and STN neurons and sparse connections between GPe, GPi, TH, and STN neurons, (b) RT network model including GPe, GPi, TH, and STN neurons and sparse connections between GPe, GPi, TH, and STN neurons

Membrane potential for TH, STN, Gpe, and GPi neurons are according to Equations 1, 2, and 3, respectively. The numerical values of the parameters and equations of the BG and RT models, as well as the differences between the BG and RT models, have been selected from reference [28].

$$C_m V' = -I_L - I_{Na} - I_K - I_T - I_{GPi\to Th} + I_{SMC} \qquad (1)$$

$$C_m V' = -I_L - I_{Na} - I_K - I_T - I_{Ca} - I_{ahp} - I_{GPe\to STN} + I_{app} + I_{dbs}\ (I_{ChR2}, I_{NpHR}) \quad (2)$$

$$C_m V' = -I_L - I_{Na} - I_K - I_T - I_{Ca} - I_{ahp} - I_{STN\to GP} + I_{GPe\to GPe/GPi} + I_{app} + I_{dbs}\ (I_{ChR2}, I_{NpHR}) \quad (3)$$

Where I_{dbs} is the current of electrical stimulation called Deep Brain Stimulation (DBS). Since we did not apply DBS, then we supposed it equal to zero ($I_{dbs} = 0$). I_{SMC} is SMC input to TH cells, I_{ChR2} and I_{NpHR} are optical currents. Membrane currents of leak current (I_L), fast Na and K currents (I_{Na}, I_K), Ca currents (I_{Ca}, I_T), and Ca-activated voltage-independent K-current (I_{ahp}) are as Equations 4-9.

$$I_L = g_L(v - E_L) \quad (4)$$

$$I_{Na} = g_{Na} m_\infty(v)^3 h\,(v - E_{Na}) \quad (5)$$

$$I_K = gKn^4\,(v - E_k) \quad (6)$$

$$I_{Ca} = gca\, s_\infty(v)^3 (v - E_{Ca}) \quad (7)$$

$$I_T = g_T a_\infty(v)^3 b_\infty(r)^2 r(v - E_T) \quad (8)$$

$$I_{ahp} = g_{ahp}(v - E_{ahp})\left(\frac{CA}{CA + k_1}\right) \quad (9)$$

Parameters of m_∞, a_∞ and s_∞ are immediate voltage-dependent gating variables, b_∞ is a sigmoidal function of time dependent variable r. the concentration of intracellular Ca^{2+} has been administered by calcium balance ($\frac{dCA}{dt} = \varepsilon(-I_{Ca} - I_T - k_{Ca} \times CA)$). Gating variables of n, h, and r have been explained by $\frac{dx}{dt} = (x_\infty(V) - x)/\tau(V)$. the connection between network components (inhibitory and excitatory synapses) have been modeled by equation ($\frac{ds}{dt} = \alpha H_\infty(V_{presyn} - \theta_g)(1 - s) - \beta s$) for a segment of activated channels, which H_∞ is equal to $H_\infty(V) = 1/(1 + exp\,[-(V - \Theta_g^H)/\sigma_g^H]$). Synaptic currents (I_{syn}) of $I_{GPi\to Th}, I_{GPe\to STN}, I_{STN\to GP}$, and $I_{GPe\to GPe/GPi}$ have been defined as equation $I_{syn} = g_{syn}(V - V_{syn})\sum_j S_j$ [28] where g_{syn} is synaptic stretch connections between neurons, V is membrane potentials of cells, and V_{syn} is synaptic voltage of cells.

2.2. Sensorimotor Cortex Input (SMC)

The sensory-motor cortex is a region of the brain that includes the precentral and postcentral gyri and includes the primary sensory and motor area of the brain, which was first introduced by Munk [33] in 1881. He called this part, which is located in a large area in the visual and auditory centers of the brain, the sensory sphere. The sensory-motor cortex contains neurons that play a role in movement control. The thalamus is also composed of different nuclei, each of which plays a unique role, including receiving and transmitting sensory and motor signals in the form of impulses from the sensory-motor cortex of the brain [33, 34]. Therefore, SMC is a signal input from the sensory-motor cortex to the thalamus [28] and in all the modeling references of brain neurons, it is considered as current pulses, which are sent to TH neurons as shown in Figure 1a, 1b. As in Equation 1, this signal input is defined as I_SMC current and describes the sensory-motor cortex input to TH neurons.

Therefore, I_{SMC} is modeled as monophasic pulses (in the form of a train of pulses) with Equation 10 [32] with the amplitude of $i_{SM} = 3.5uA/cm^2 = 0.035pA/\mu m^2$, the pulse width of $\delta_{SM} = 0.3ms$ and stimulation period of $\rho_{SM} = 7.7ms$ with Heaviside step of H is applied to evoke an action potential with each pulse to TH neurons.

$$I_{SM} = i_{SM} H\left(sin\left(\frac{2\pi t}{\rho_{SM}}\right)\right)[1 - H\left(sin\left(\frac{2\pi(t + \delta_{SM})}{\rho_{SM}}\right)\right) \quad (10)$$

2.3. ChR2-Expression

In this paper, we have considered ChR2 (ChRwt, ChETA) as a light-sensitive opsin and applied it to the BG and RT network model. ChR2 is a light-sensitive sodium channel for stimulating neurons by depolarizing neurons [19]. In order for this current to be comparable with previous theoretical studies and valid experiments, the current (ChR2) ((I_{ChR2}) in the form of pulses with a frequency of 100 Hz, a pulse width of 5 ms, and a stimulation period of 10 ms with a number of 15 pulses (the same as in reference [29]). In general, two computational models have been proposed to model opsins, and based on this, we have also used these two models to check the results: the three-state model [35] and the four-state model [23, 36].

2.3.1. Three-State Model

The three-state model is successful in predicting the peak and steady state of the current and for analyzing

the fast movement of ChR2. Provides a simple analysis mode that supports the calculation of deactivation and recovery time constants for optical currents. The three-stage model includes open stages (O), closed stages (C), and dark transition stages (D) Figure 2. Also, c, o, and d are a fraction of ChR2. The c is removed from the equation because the relation c+o+d=1 is established. The dynamics of the transitions between states have been described as Equation 11 and Equation 12 [29].

$$\dot{O} = \varepsilon F Q(t)(1 - o - d) - G_{do} \quad (11)$$

$$\dot{d} = G_{do} - G_{rd} \quad (12)$$

$$F = \sigma_{ret} \frac{\varphi}{w_{Loss}} \quad (13)$$

$$\varphi = \frac{\lambda A}{hc} \quad (14)$$

$$A(t) = A_{light} \emptyset(t) \quad (15)$$

$$I_{ChR2} = g_{ChR2} VO \quad (16)$$

The number of photons absorbed by ChR2 molecules per time unit is as Equation 13 [27], where σ_{ret} is the cross-sectional area of the network equal to the value of $\sigma_{ret} = 1.2 \times 10^{-20} m^2$. w_{Loss} is the loss of photon due to absorption and scattering. Photon flux per area is defined as Equation 14, where λ is the excitation wavelength of blue light equal to 480 nm, A is the intensity of the stimulation light, c is the speed of light, and h is Planck's constant [34]. Light pulses are applied as Equation 15. According to studies, damage to the superficial cortical tissue occurs $A > 100 mw/mm^2$. While light intensities of $A < 75 mw/mm^2$ are sufficient to evoke neural activation. Also, pulsed radiation reduces tissue damage compared to continuous radiation [37]. ChR2 photocurrent is defined as Equation 16, V is the membrane potential for ChR2.

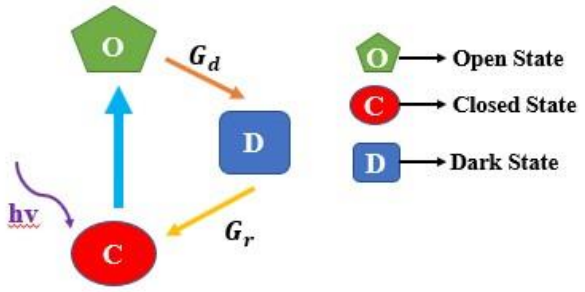

Figure 2. Photocycle model for Dynamics of three-state optogenetic stimulation

The three-mode excitation parameter values are from reference [29] and are presented in Table 1.

Table 1. Parameters values and descriptions for three-state Optogenetics

Parameter	Parameters description	Value
ε	Transition tare for O state	0.4296 ms^{-1}
G_r	Transition tare for D → C	0.1385 ms^{-1}
G_d	Transition tare for O → D	0.6518 ms^{-1}
σ_{ret}	Retinal cross-section	$1.2*10^{-2}$ m^2
h	Planck's constant	$6.63*10^{-36}$ Js
c	Speed of light	$3*10^8$ m/s
λ	Wave length of the light	570nm
g_{NpHR}	Maximum conductance of NpHR in O state	2.4002 nS/ **μm²**

2.3.2. Four-State Model

In this case, a four-step transition for ChR2, which is the fastest optical flow, has been considered to follow the photo stimulation movement Figure 3. Two open stages include O1 and O2 and two closed stages include C1 and C2. It should be noted that the open and closed stages are internal transition stages. The dynamics of transitions between stages are in the form of Equations 17-20 [29]:

$$\dot{O}_1 = \varepsilon_1 uF\,(1 - c_2 - o_1 - o_2) - (G_{d1} + e_{12})o_1 + e_{21}o_2 \quad (17)$$

$$\dot{O}_2 = \varepsilon_2 uFc_2 + e_{12}o_1 - (G_{d2} + e_{21})o_2 \quad (18)$$

$$\dot{C}_2 = G_{d2}o_2 - (P_2 u + G_r)c_2 \quad (19)$$

$$\dot{u} = (S_0\,(Q) - u)/\tau_{ChR2} \quad (20)$$

c1, c2, o1 and o2 show the fraction of ChR2 molecules in C1, C2, O1 and O2 stages. ε_1, ε_2, G_{d1}, G_{d2}, e_{12}, e_{21} and G_r are transfer rates. τ_{ChR2} expresses the activity time of the ChR2 ion and is equal to 1.5855 ms. P_2 is excitation rate. For c_1, due to the existence of Equation 21, a relation is not considered.

$$c1 + c2 + o1 + o2 = 1 \quad (21)$$

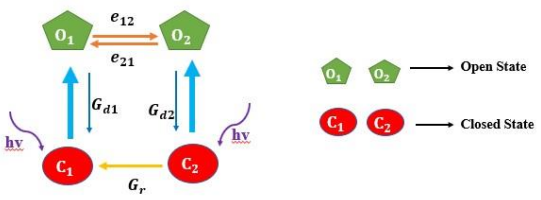

Figure 3. Photocycle model for Dynamics of four-state optogenetic stimulation

ChR2 molecules initially are in closed state C1, then by irradiating light they transmit to open state O1 and by continuing irradiation to open state of O2 that has less conductivity than O1 or they return to C1. So, they go again to O1 or C2. When the light turns off, they return to the C1 state slowly [36, 38]. u function is referred to temporal kinetics of the conformational change in protein. The number of photons absorbed by ChR2 in per unite of time is $\mathrm{F} = \sigma_{\mathrm{ret}} \frac{\varphi}{\mathrm{w_{Loss}}}$ [27].

Where $\sigma_{\mathrm{ret}} = 1.2 \times 10^{-20} m^2$ is the retinal cross-section and $w_{loss}$is the loss of photon due to absorption and scattering. φ is the photon leak per area $\varphi = \lambda A/hc$, in which $\lambda = 480\, nm$ is blue light wavelength, A is the intensity of light stimulation, h is Plank's constant, and c is the speed of light [34]. According to the recent represented reports, damage to superficial cortex tissue occurs in $A > 100\, mw/mm^2$.

However, light intensities of $A < 75\, mw/mm^2$ is sufficient to evoke neural activation. Also, pulse irradiation (pu) reduces tissue damage to continue irradiation (cw) [34]. Sigmoidal function is as Equation 22 in which ∅(t) describes the protocol of stimulation, Equation 23.

$$S_0(\emptyset) = 0.5\,(1 + tanh(120(\emptyset - 0.1)) \quad (22)$$

$$\emptyset(t) = \Theta(mod(t, P) - t_{off} \quad (23)$$

Where Θ is the Heaviside function, P is the period of stimulation, $\mathrm{t_{off}}$ is the time per cycle when the stimulation is off. Pulse duration has been defined as Equation 24. Light pulses are considered Equation 25, A_{light} is the constant light intensity.

$$t_{on} = p - t_{off} \quad (24)$$

$$A(t) = A_{light}\emptyset(t) \quad (25)$$

$$I_{ChR2} = g_{ChR2}(V - V_{Na})(O_1 + \gamma O_2) \quad (26)$$

ChR2 photocurrent is defined as Equation 26. Since the values were selected according to reference [29], to compare and analysis of the studies of the ChR2 current $\mathrm{I_{ChR2}}$ as pulses with a frequency of 100 Hz, pulse duration of 5 ms, and period of stimulation is 10ms. $\mathrm{g_{ChR2}}$ is the maximum conductance of ChR2 in $\mathrm{O_1}$ state, $\mathrm{V_{Na}}$ is a reversal potential of sodium and γ is the conductance rate in the $\mathrm{O_1}$ and $\mathrm{O_2}$ states [29]. The values of four-state stimulation parameters have been inserted from [29] reference and represented in Table 2.

Table 2. Parameters values and descriptions for four-state Optogenetics

Parameter	Parameters description	Value
ε_1	Transition rate of O1 state	4.6125 ms^{-1}
ε_2	Transition rate of O2 state	2.1969 ms^{-1}
$\mathrm{G_{d1}}$	Transition rate for O1 → C1	0.1779 ms^{-1}
$\mathrm{G_{d2}}$	Transition tare for O2 → C2	0.2362 ms^{-1}
$\mathrm{G_r}$	Recovery rate of C1 after the light pulse turned off	0.004 ms^{-1}
$\mathrm{e_{12}}$	Transition rate for O1 → O2	0.0696 ms^{-1}
$\mathrm{e_{21}}$	Transition rate for O2 → O1	0.0268 ms^{-1}
τ_{ChR2}	Activation time of the ChETA ion channel	1.5855 m^2
σ_{ret}	Retinal cross-section	$1.2*10^{-2}$ m^2
h	Planck's constant	$6.63\text{-}10^{-36}$ Js
c	Speed of light	$3*10^8$ m/s
λ	Wave length of the light	480 nm
g_{ChR2}	maximum conductance of ChETA in $\mathrm{O_1}$ state	0.8755 nS/μm^2

2.4. NpHR-Expression

In this case, the NpHR opsin, the chlorine pump activated by yellow light with a wavelength of 570 nm, has been chosen to stop neuronal activity with hyperpolarization [39]. Current NpHR ($\mathrm{I_{NpHR}}$) is as pulses with a frequency of 100 Hz, pulse width of 5 ms, and a stimulation period of 10 ms with a number of 15 pulses.

2.5. Network Performance Evaluation

In this paper, the response of neurons of both BG and RT network models for different short and long stimulations of three-state optogenetic models ChETA, three-state ChRwt, four-state ChETA, four-state ChRwt, and NpHR have been analyzed and compared with experimental and theoretical results

presented in reliable sources. In this paper, we have considered and analyzed the response (spike or action potential) of neurons of the basal ganglia (TH, GPi, GPe, and STN). Since the recording of these neuronal responses requires electrodes to be placed deep in the deep areas of the brain and the Local Field Potential (LFP) of these neurons should be extracted, so doing this type of test on humans and access to this information through EEG signal or tomographic images is not possible. On the other hand, human or animal samples recorded from the response of the basal ganglia neurons in references in the field of stimulation Optogenetics with the selection of different opsins for comparison are not available.

In experimental and theory references, each neuron with differential equations Hodgkin-Huxley or WB modeled, and by solving these equations for all neurons they have reached to spiking responses of neurons [19, 27]. The first source of theoretical studies to which we have compared our results related to Honghui Zhang *et al.* (2020) [19], who have investigated neural opto stimulation to model the firing activities of GPe neurons related to the basal ganglia to estimate and evaluate treatment methods for neurological disorders such as Parkinson's disease.

For this purpose, three-state and four-state optogenetic stimulation models were used computationally and theoretically with the application of different opsins ChETA, ChRwt, and NpHR, and only the response of GPe neurons based on the Hodgkin-Huxley model to each stimulation have been investigated. The second source of experimental studies that have been considered to compare the results is related to Roxana *et al.* (2013) [27], first, they introduced and investigated three and four-state optogenetic models experimentally by applying different parameters and different ChRwt and ChETA opsins obtained from experimental data [40, 41].

Then, with three-state and four-state stimulation models presented as experimentally, only the response of GPe neurons based on the WB [42] model has been analyzed computationally by applying different light stimulation protocols and different opsins. The process of recording the neuronal responses in vitro, outside the body of the living organism, with the patch-clamp method of the parvalbumin neurons of the hippocampus of the rat brain, was performed by injecting the virus within 2-3 weeks.

The stimulation conditions include the application of 470 nm blue light with a light intensity of 1.4 mw/mm^{2}and pulse width of 2 ms at a constant voltage of -60 mV with frequencies of 10, 80, and 200 Hz, and the selected opsins are ChETA and ChRwt. Examples of the results obtained in two sources [19] and [28] for two three-state models with ChETA opsin and four-state ChRwt model with frequencies f=10-200 Hz and the number of pulses ns=3-40 have been shown respectively in Figure 4 (a, b). Based on the results of the GPe neurons of the three-state ChETA model presented in Figure 4a, there is one response for each stimulation at the frequency of 10 Hz, and for the frequencies of 80 and 200 Hz, the responses to the stimulation are lost. This means that similar to the circular box in Figure 4a, for some red pulses related to optogenetic stimulation, neurons have no response signal or action potential. The results for GPe neurons for the four-state ChRwt model in Figure 4b show that for all frequencies (f=10-200 Hz) and number of pulses (ns=3-40), the responses for each stimulation as an additional response, similar to the oval box in Figure 4b, for each blue pulse related to optogenetic stimulation, neurons generate two or more responses or action potentials. In addition, for high frequency (200 Hz) Plateau Potential, which is actually a membrane potential depolarization that is maintained by intrinsic properties even after the end of stimulation, arises, which is one of the characteristics of ChRwt opsin. This potential does not exist for ChETA and has not been reported [19, 27].

In these Figures, we have tried to show the four states of responses with different symbols and categorize them so that the missing response with a symbol of a circular box, an additional answer with the symbol of an oval box, for each stimulus, a response is marked with a rectangular symbol and the plateau potential with a dashed rectangle have been represented. BG and RT network performance has been investigated by measuring how TH neurons respond to SMC input by considering EI. The error index described by Rubin and 2002 [32] gives a quantitative measure of the accuracy of TH performance [28]. The network achieves optimal performance when each SMC input pulse generates an action potential in TH neurons. The voltage across the membrane surface has been considered to be -40 mV. Three types of errors have been considered for TH neurons as spurious, bursting, and missing events.

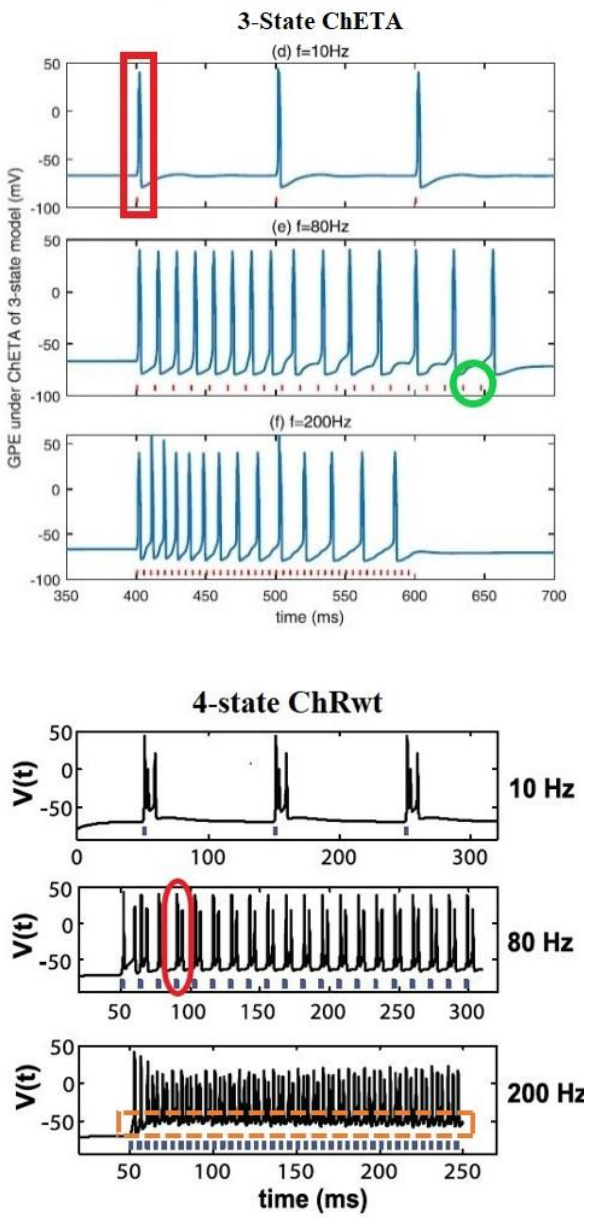

Figure 4. The response of GPe neurons to stimulation for frequencies f=10-200Hz and a number of pulses ns=3-40, a) ChETA three-state model [18], b) ChRwt four-state model [27]. (The rectangular box is for one response for each stimulation, the circular box is for the missing response, the oval box is for the additional response, and the dashed rectangular box is for the plateau potential

The error index is defined by Equation 27, where N_{miss} is the number of missed errors, N_{burst} is the number of burst errors, and N_{spur} is the number of spurious event errors of TH neurons in response to SMC input, (the error values are from the firing rate graph of TH neurons as has been shown in Figure 5 [43]. Therefore, EI is the value of the wrong response to the input pulses from the SMC relative to the total number of inputs of the SMC (N_{SM}, which we have considered its value in our simulations based on Fan *et al.* [41], equal to 16) which describes the incorrect operation of TH. Miss (*), exists when one neuron can not evoke an action potential. Burst (^), happens when a neuron evokes more than one for one pulse of SMC input during 25 ms. Spurious occurs when a TH cell evokes without stimulation.

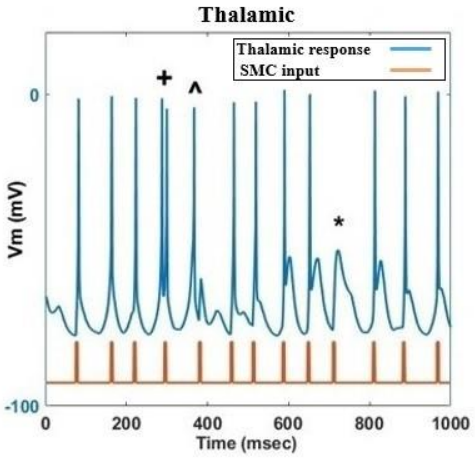

Figure 5. An example of TH neurons response to SMS, *: represents miss error, +: represents burst error and ^ : represents spurious error

$$EI = \frac{N_{miss} + N_{burst} + N_{spur}}{N_{SM}} \quad (27)$$

3. Results

3.1. Results of Different Short Stimulations for the BG and RT Network Models of the ChR2 Optogenetic Model

3.1.1. Results of ChETA Three-State Model on BG Network Model

In this part, we have calculated the response of GPe, GPi, and STN neurons to the ChETA three-state model for the BG network model and the response of TH neurons to input from SMC with frequencies of f=10-200 Hz, number of pulses of ns=3-40 and the pulse width of ton =2ms and depicted the results in Figure 6 (a, b, and c). To measure the correctness of the results of the presented model, we have tried the selected parameters (ton, ns, f that in Figure 6 has been considered) to match with the considered experimental and computational parameters.

For this purpose, the response of GPe neurons to three-state stimulation of ChETA related to reference [19] for f=80,200 Hz and ns=20,40 in comparison with the results reported in Figure 6d has been given. Since the available experimental and computational references only have represented the responses of the GPe neurons, the results have been compared with these neurons. To further study and development of the model, considering that the model presented in this paper included other neurons (TH, GPi, and STN), we have considered the results of these cells. We have also examined neurons. As it can be seen, at f=10 Hz for GPe and GPi neurons for each stimulation there are additional spikes which are more for GPi than GPe. For STN, for each stimulation, the response with additional spikes and missing responses can be seen.

For TH neurons, there is one response for each stimulation along with two additional responses (two burst errors) (Figure 6a). At f=80Hz, the number of missed responses is high for STN and GPe neurons, but it is low in GPi, and TH neurons have one error-free response to each stimulation. At this frequency, the lost response of GPe neurons can be seen, which is consistent with the experimental results [19] (according to the results of Figure 6b, which has been shown with a green circular box). At f=200Hz, GPi and TH neurons respond to every stimulation and the number of missed responses is low, but in STN and GPe neurons, the number of missed responses is high. Therefore, the response of GPe neurons in the form of a missing response is comparable to the experimental results [19] (Figure 6c which is marked with a green circular box.). Also, the absence of Plateau potential for ChETA at high frequency (200 Hz) also shows its conformity with the existing valid experimental results [19, 27]. It should be noted that the results related to other neurons are similar to the results of GPe neurons. Based on the obtained results, in this model, the frequency of 80 Hz with 20 pulses and EI=0 is optimal for f and ns.

3.1.2. Results of ChETA Three-State Model on RT Network Model

By applying ChETA three-state stimulation to the RT network model, we have calculated the response of GPi, GPe and STN neurons and the output of TH neurons to the input from SMC with f=10-200Hz, ns=3-40, and ton=2 ms and have reported the results

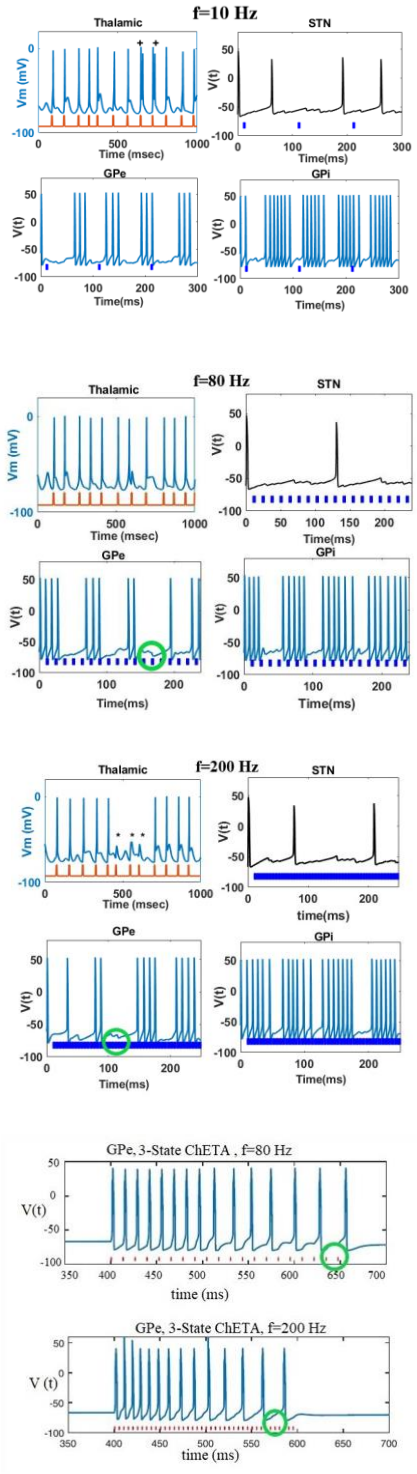

Figure 6. Response of GPe, Gpi, and STN neurons to ChETA three-state model for BG network model and TH response to SMC, (a) f=10 Hz, ns=3, t_{on}=2 ms , (b) f=80Hz, ns =20, t_{on}=2 ms, (c) f=200 Hz, ns=40, t_{on}=2 ms, (d) response of GPe neurons to stimulation for f=80,200Hz and ns=20,40 to ChETA three-state model [19]. (The circular boxes indicate the missing answer.). (Orange pulses at TH output correspond to SMC input pulses, blue pulses at GPi, Gpe, and STN outputs are for ChETA three-mode stimulation light pulses and red pulses at the output of GPe neurons are for ChETA three-state stimulation light pulses for the experimental and computational results [19]

in Figure 7 (a, b and c). To validate the results of the presented model, we have tried to make the selected parameters (ton, ns, f specified in Figure 7) match with the experimental and computational parameters of the desired sources. To compare the reported results, we have presented the response of GPe neurons to three-state ChETA stimulation in reference [19] for f=80,200 Hz and ns=20,40 in Figure 7d. Comparing the response of neurons with GPe shows that at frequency f=10 Hz for GPi and GPe neurons, there are additional responses for each stimulation, which is more for GPi and for STN, the response is in the form of additional, and inhibitory spikes.

For TH neurons, a response with an additional spike (a burst error) is seen for each stimulation (Figure 7a). At f=80Hz, the number of lost responses is high for GPi, GPe and STN neurons. The response of GPe neurons is consistent with the experimental results [19] that the responses are suppressed and lost (according to the results of Figure 7b which is indicated by a green circular box). For TH neurons, there is one error-free response for each stimulus. At f=200Hz, the number of missed responses is high for GPi, Gpe, and STN neurons. For TH neurons, one response is seen for each stimulus along with an additional response with a burst error. The absence of plateau potential for ChETA at high frequency (200 Hz) shows its agreement with the existing experimental and computational results [19, 27], therefore, at this frequency, the response of GPe neurons is consistent with the experimental results [19] (Figure 7c which is marked with a green circular box) and the results for other neurons are similar to the GPe results. In Table 3, the results and response of the BG and RT network model neurons (TH, GPe, Gpi, and STN) to the stimulation of the three-state ChETA model for different parameters (A, ns, f, ton) are presented, considering EI and the compatibility of the results with the existing experimental and computational results has been checked. According to the obtained results, in this model, the frequency of 80 Hz with 20 pulses and EI=0 is optimal f and ns.

3.1.3. Results of ChRwt Three-State Model on BG Network Model

The output of GPe, GPi, and STN neurons to ChRwt three-state model for the BG network model and the output of TH neurons to the SMC input with frequencies of f=10-200 Hz, number of pulses of ns=3-40 and the pulse width of ton =2ms has been considered and the results has been depicted in Figure 8(a, b and c). For verification, it has been tried again that the selected parameters ton, ns, f, Figure 8, are consistent with the experimental and computational parameters of the considered resources.

To reach this goal, the output of GPe neurons to the stimulation of the three-state model ChRwt related to reference [19] for f=10,200 Hz and ns=3,40 has been shown in Figure 8d. According to the comparison of the results with the results obtained from GPe neurons, at a frequency of 10 Hz for GPe and GPi neurons, responses with additional spikes can be seen for each stimulation, so the response with additional spikes for GPe neurons is in accordance with the experimental results [19, 27] (as in Figure 8a which is marked with a red oval box).The output of STN and TH neurons is accompanied by an additional and missing response, and for TH there are two misses and one burst errors. At the frequency of 80 Hz, the missing response can be seen for GPe, GPi and STN neurons, and there are additional spikes for TH neurons (three burst errors) (Figure 8a). At the frequency of 200 Hz, the response of GPe, GPi and STN neurons is lost and there is no Plateau potential. For TH neurons, there is one response for each stimulation, except for two cases that are suppressed (two miss errors). According to the experimental results [19], the response of GPe neurons is lost and without a Plateau potential, in the presented model corresponds to the response of GPe neurons, which is missing and does not have a plateau potential (according to the results of Figure 8c, which is shown with a green circular box). The results show that the responses of other neurons are similar to the results of GPe. In this model, the frequency of 200 Hz with the number of pulses is 40 with the lowest value for EI are as the optimal frequency and number of pulses.

3.1.4. Results of ChRwt Three-State Model on RT Network Model

We have applied ChRwt three-state stimulation with frequencies of f=10-200Hz, number of pulses of ns=3-40 and pulse width of t_{on}=2ms to the RT network model. We have presented the response of GPe, GPi and STN neurons as well as the response of TH neurons to SMC input in Figure 9 (a, b and c).

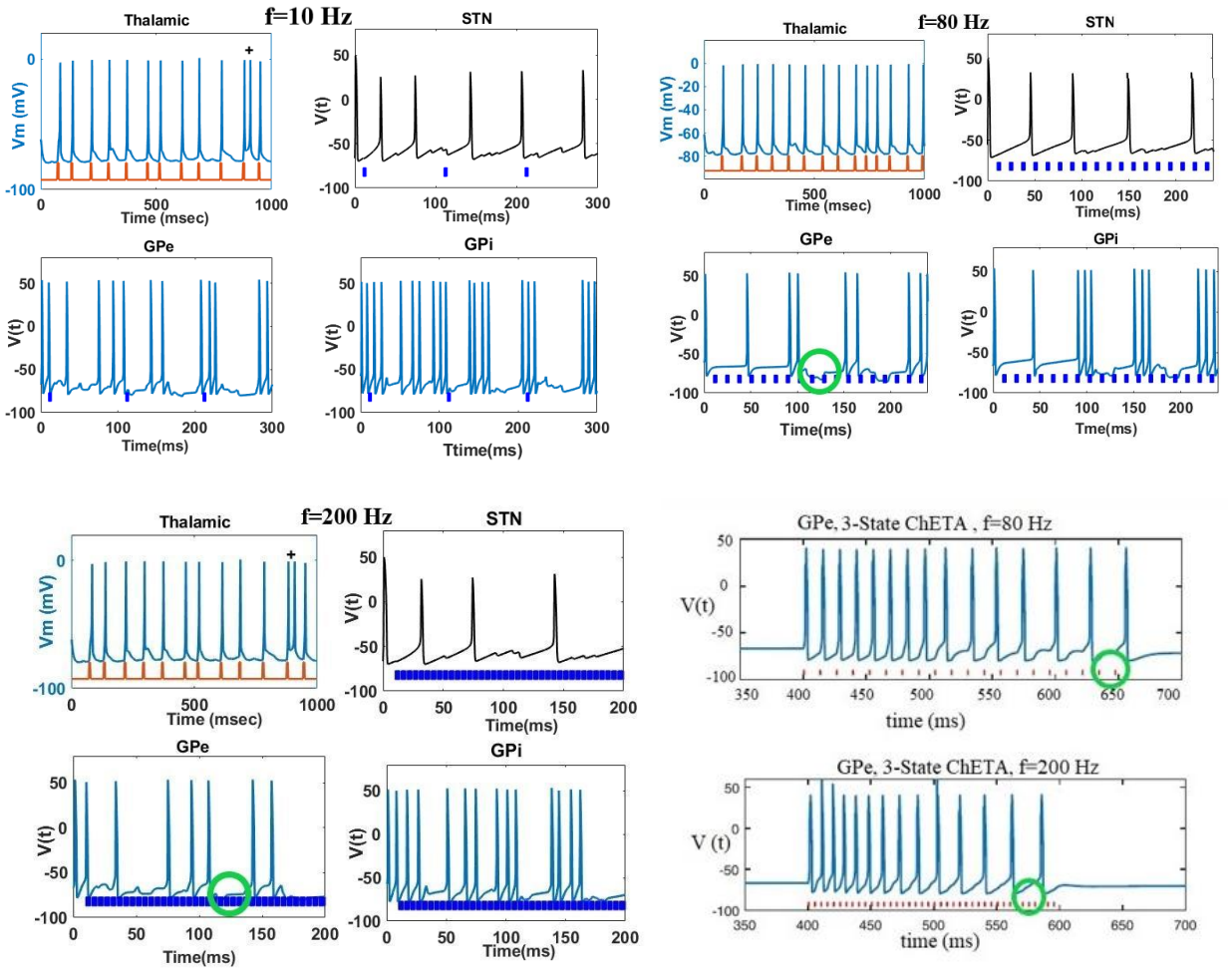

Figure 7. Response of GPe, GPi and STN neurons to ChETA three-state model for RT network model and TH response to SMC (a)f=10 Hz, ns=3, t_{on}=2 ms , (b) f=80Hz, ns=20, t_{on} =2 ms , (c) f=200 Hz, ns=40, t_{on} =2 ms,(d) response of GPe neurons to stimulation for f=80,200Hz and ns=20,40 to the ChETA three-state model [19] (circular boxes are for missing response). (Orange pulses at TH output correspond to SMC input pulses, blue pulses at GPi, GPe and STN outputs are for ChETA three-state stimulation light pulses and red pulses at the output of GPe neurons are for ChETA three-state stimulation light pulses for the experimental and computational results [19]

Table 3. Results and responses of BG and RT network model neurons (STN, GPe, GPi, TH) to stimulation of ChETA three-state model with different parameters (A, ns, f, ton)

EI	Response of TH	Response of STN	Response of GPe	Response of GPi	A(mw/mm^2)	n s	t_{on} (ms)	f (Hz)	Optogenetic model
0.12	For each stimulus a response with an additional response	Additional spike and missing response	Additional spike	Additional spike	50	3	2	10	Three-state ChETA BG
0	One response for each stimulus	Missing response	Missing response [19]	Missing response	50	20	2	80	
0.18	Few answers are missing	Missing response	Missing response and lack of Plateau potential [19, 27]	Few answers are missing	50	40	2	200	
0.06	One response for each stimulus	Additional spike and missing response	Additional spike	Additional spike	50	3	2	10	Three-state ChETA RT
0	One response for each stimulus	Missing response	Missing response [19]	Missing response	50	20	2	80	
0.06	One response for each stimulus with additional spike	Missing response	Missing response and lack of Plateau potential [19,27]	Missing response	50	40	2	200	

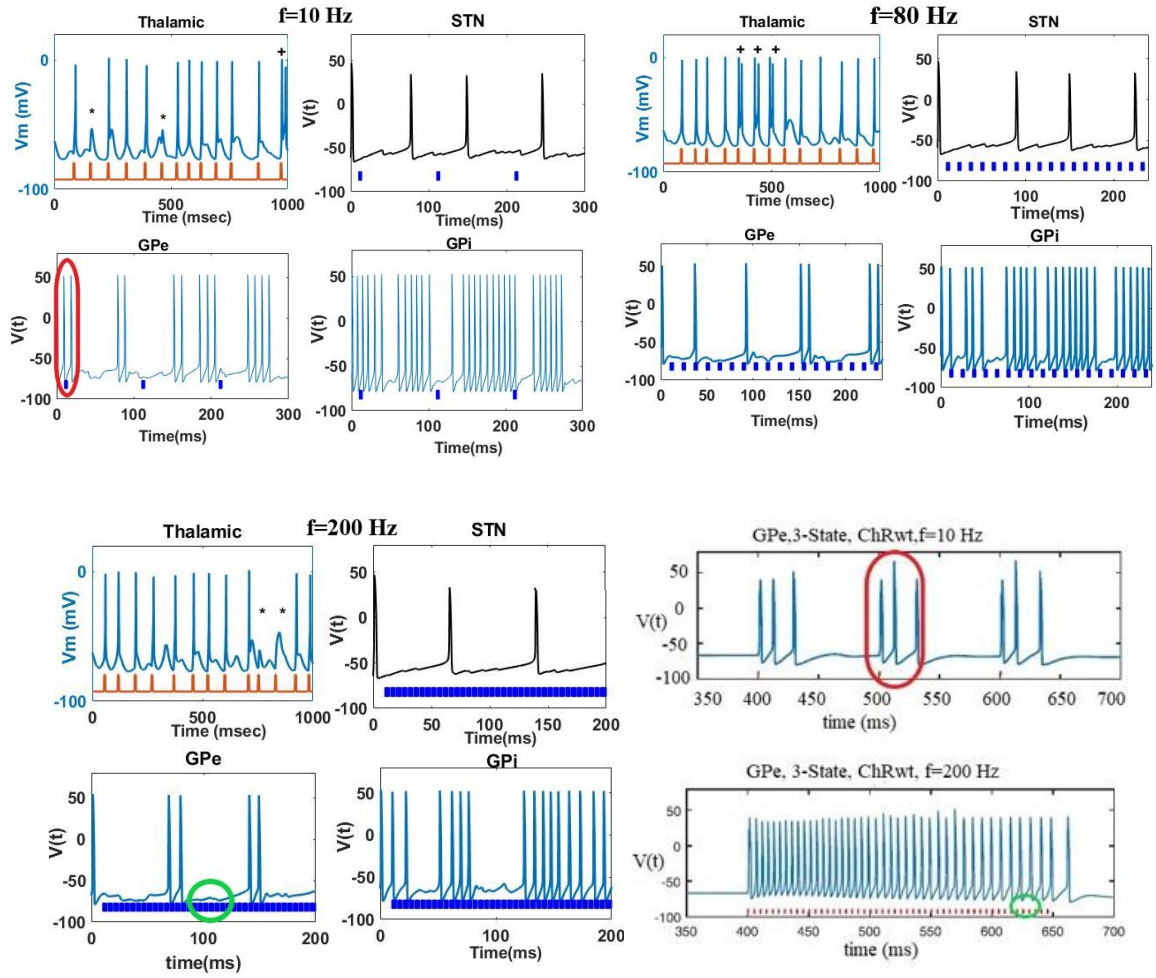

Figure 8. Response of GPe, Gpi, and STN neurons to ChRwt three-state model for BG network model and TH response to SMC (a).f=10 Hz, ns=3, t_{on}=2 ms, (b)f=80Hz, ns=20, t_{on} =2 ms. (c)f =200 Hz, ns=40, t_{on} =2 ms, (d) Response of GPe neurons to stimulation for f=10,200Hz and ns=3,40 to ChRwt three-state model [19] (oval box indicates additional response and circular box for response are lost). (Orange pulses at TH output correspond to SMC input pulses, blue pulses at GPi, Gpe, and STN outputs are for ChRwt three-state stimulation light pulses and red pulses at the output of GPe neurons are for ChRwt three-state stimulation light pulses for the experimental and computational results [19]

Also, in order to verify the accuracy, we have chosen the parameters t_{on}, ns, f, Figure 9, according to the experimental and calculation results of the considered sources. From comparing the response of neurons with the results of GPe neurons an example of the response of these neurons (GPe) to the stimulation of the ChRwt three-state model related to reference [19] for frequencies of 10 and 200 Hz with the number of pulses 3 and 40 in Figure 9, it can be seen that, at f=10 Hz for GPe and GPi neurons, responses with additional spikes can be seen for each stimulation, and the response for GPe is in accordance with the experimental results [19, 27] (as shown in Figure 9a which is marked with a red oval box). The response of STN neurons is additional and missing, and for TH there is one error-free response per stimulation. At frequencies of 80 and 200 Hz, (Figure 9b and 9c), for each stimulation, the response of GPe, Gpi, and STN neurons is suppressed and lost, and no Plateau potential is seen at 200 Hz. Therefore, at the frequency of 200 Hz, the response of GPe neurons, which is lost and does not have a plateau potential, is in accordance with the experimental results [19] (according to the results of Figure 9c, which is marked with a green circular box). For TH neurons, additional spikes (one burst error) and additional responses (three bursts) are observed at 200 Hz. According to the results, the responses of other neurons are similar to the GPe results.

In Table 4, the results and responses of the BG and RT network model neurons (TH, GPe, Gpi, and STN)

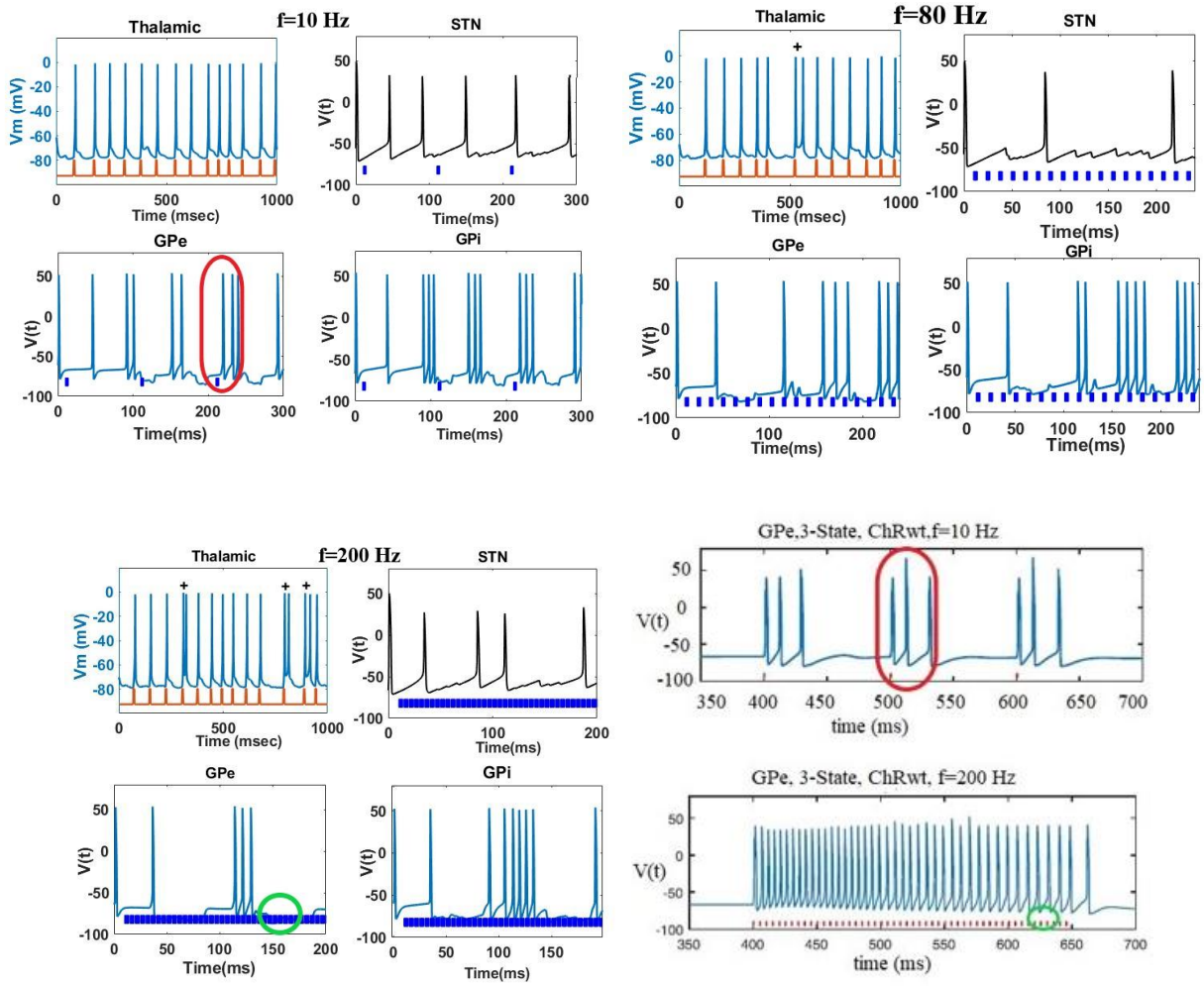

Figure 9. Response of GPe, Gpi, and STN neurons to ChRwt three-mode model for RT network model TH response to SMC (a) f=10 Hz, ns=3, t_{on}=2 ms, (b)f=80Hz, ns=20, t_{on}=2 ms, (c) f=200 Hz, ns=40, t_{on}=2 ms, (d) response of GPe neurons to stimulation for f=10,200Hz and ns=3,40 to ChRwt three- state model [19] (oval boxes indicate additional response and circular box for missing response.). (Orange pulses at TH output correspond to SMC input pulses, blue pulses at GPi, Gpe, and STN outputs are ChRwt three-state model stimulation light pulses, and red pulses at the output of GPe neurons are for ChRwt three-state stimulation light pulses for the experimental and calculation results [19])

Table 4. Results and responses of BG and RT network model neurons (STN, GPe, GPi, TH) to stimulation of ChRwt three-state model with different parameters (A, ns, f, ton)

EI	Response of TH	Response of STN	Response of GPe	Response of GPi	A (mw/mm^2)	ns	t_{on} ms	f Hz	Optogenetic model
0.18	Additional spike and missing response	Additional spike and missing response	Additional spike [19, 27]	Additional spike	50	3	2	10	
0.18	Additional spike	Missing response	Missing response	Missing response	50	20	2	80	Three-state ChRwt BG
0.12	Missing response	Missing response	Missing response and lack of Plateau potential [19]	Missing response	50	40	2	200	
0	One response for each stimulus	Additional spike and missing response	Additional spike [19, 27]	Additional spike	50	3	2	10	
0.06	Additional spike	Missing response	Missing response	Missing response	50	20	2	80	Three-state ChRwt RT
0.18	Additional spike	Missing response	Missing response and lack of Plateau potential [19]	Missing response	50	40	2	200	

to the stimulation of the ChRwt three-state model for different parameters (A, ns, f, t_{on}) are presented considering EI and the same results are observed with the existing experimental and computational results. Based on these results, in this model, the frequency of 10 Hz with the number of pulses 3 and EI=0 is considered as the optimal frequency and number of pulses.

3.1.5. Results of ChETA Four-State Model on BG Network Model

In this section, we have tested the output of GPe, Gpi, and STN neurons by applying the ChETA four-state stimulation for the BG network model, as well as the output of TH neurons to the SMC input due to frequencies of f=10-200Hz with the number of pulses ns=3 -40 and the pulse width of ton = 2ms have been analyzed and the results have been shown in Figure 10 (a, b, and c). For the correctness of the study, we have chosen the same parameters as the experimental and calculation parameters, which are specified as ton, ns, and f in Figure 10. By comparing the results of the neurons with the response of the GPe neurons, it can be seen that, at f=10Hz, for all three GPe, Gpi, and STN neurons, additional responses are produced for each stimulation, and for TH neurons, except in three cases that the responses are in the form of missed (three miss errors), there is one response for each stimulus (Figure 10a). At f=80Hz, the response is less for STN and TH neurons, and TH has two miss errors, but the number of responses is high for GPe and GPi neurons (Figure 10b). At f=200Hz, for GPe, GPi and STN neurons, the number of responses is less and there is no stable potential, which the lack of Plateau potential at high frequency (200Hz) is in accordance with the experimental results [19, 27] (according to Figure 10c). But in TH neurons, the number of responses does not match the stimulation in two cases, and one burst and one spurious error are seen. In this model, the frequency of 200 Hz with the number of pulses 40 and with less EI is the optimal frequency and number of pulses.

3.1.6. Results of ChETA Four-State Model on RT Network Model

We have considered the response of GPe, Gpi, and STN neurons to the ChETA four-state model in the RT network model and also the response of TH neurons to the input from SMC with f=200-10Hz, ns=3-40 and ton=2ms and have represented the results in Figure 11 (a, b and c). For the correctness of the results, we have considered the parameters in accordance with the experimental and calculation parameters of the sources, which have been shown as ton, ns, f in Figure 11. We have shown the response of GPe neurons to ChETA four-state stimulation of reference [19] for the frequency of 80 Hz with the number of pulses of 20 in Figure 11d and have compared our results with it. Comparing the responses of neurons with GPe shows that, at f=10 Hz for all three GPe, Gpi, and STN there are additional responses per stimulation and for TH neurons except in two cases (two burst errors) for each stimulation, there is one response (Figure11a). At f=80Hz, for STN neurons, the number of responses is less, for GPi, there is an additional response, and for TH, the response is high (three burst errors). For GPe neurons, there is one response for each stimulation, which is in accordance with the experimental results [18, 26]. (Same as Figure 11b which is marked with a red rectangular box.). It can be said that the results of other neurons are similar to the results of GPe. At the frequency of 200 Hz, for GPe, Gpi, and STN neurons, the number of responses is less, and for TH neurons, additional responses (two burst errors) are seen in two cases (Figure 11c). In this frequency, Plateau potential is not seen for GPe neurons, so the absence of Plateau potential at high frequency (200 Hz) is in accordance with the experimental results [19]. In Table 5, the results and responses of BG and RT network model neurons (TH, GPe, Gpi, and STN) for the stimulation of the ChETA four-state model for different parameters (A, ns, f, ton) considering EI are presented. According to the results, a frequency of 80 Hz with 20 pulses is optimal for f and ns.

3.1.7. Results of ChRwt Four-State Model on BG Network Model

In this part, by applying the ChRwt four-mode model to the BG network model, we calculated the response of GPe, Gpi, and STN neurons and the output of TH neurons to the SMC input with f=200-10Hz, ns=3-40, and ton=2ms and the results have been represented in Figure 12 (a, b, and c). In this case, the parameters ton, ns, and f, Figure 12, have been selected according to the experimental and calculation

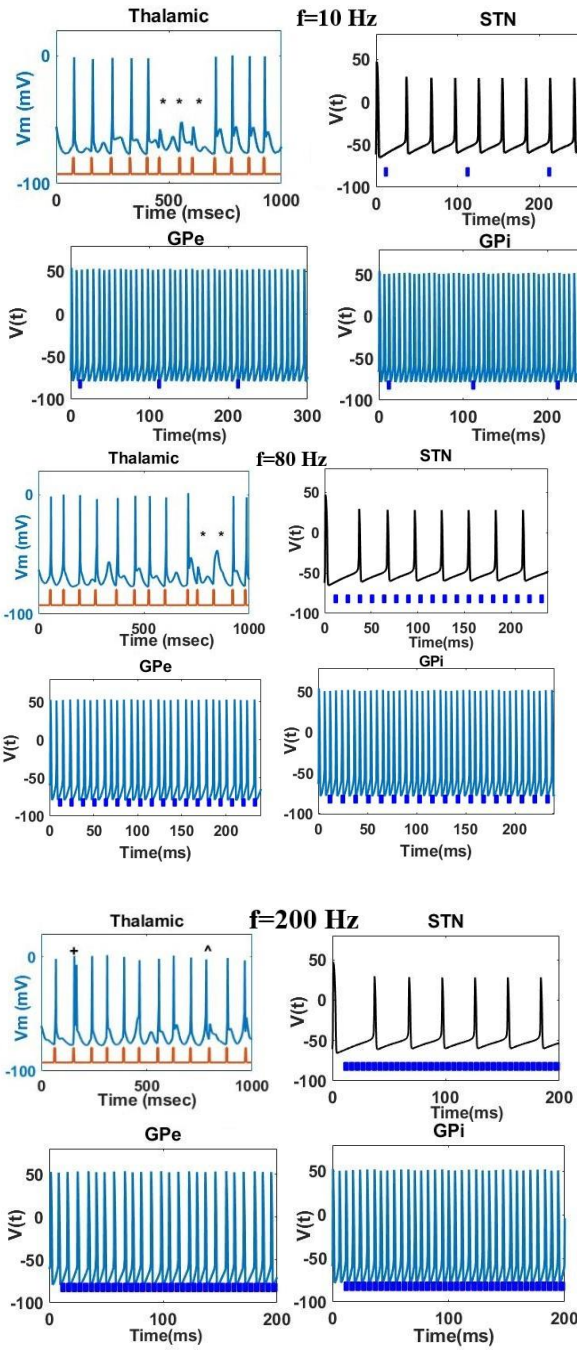

Figure 10. Response of GPe, Gpi, and STN neurons to ChETA four-state model for BG network model and TH response to SMC (a) f=10 Hz, ns=3, ton=2 ms, (b) f=80 Hz, ns=20, t_{on} = 2 ms, (c) f=200 Hz, ns=40, t_{on}=2 ms (orange pulses in the TH output are SMC input pulses, blue pulses in the GPi, Gpe, and STN outputs are the ChETA four-mode stimulation light pulses.)

parameters for the correctness of the study. The output of the neurons has been compared with the results of the GPe neurons for stimulating the ChRwt four-state related to reference [27] with f=10,80Hz and ns=3,20 which are given in Figure 12d. By comparing the outputs of the neurons with the results of GPe, it can be said that at f=10 Hz for all three neurons of GPe, Gpi, and STN, there are additional responses for each stimulation, and in this case, the results of GPe, which are in the form of additional spikes, are identical with experimental results [19, 27] (according to the results in Figure 12a, have been represented with red oval box). For TH neurons, there is one response for each stimulus, except in one case where the response is additional (a burst). At f=80 Hz, the number of responses for STN neurons is less, but for GPi and GPe, the response with additional spikes is more that for GPe neurons is in accordance with the experimental results [19, 27]. (According to the results shown in Figure 12b, with a red oval box). For TH, except in two cases where the response is additional and missing (a burst and a miss error), one response is observed for each stimulus. At f=200 Hz, for STN and GPe neurons, the number of responses is less, and for GPi, there is almost one response for each stimulus, and there is no plateau potential, and for TH neurons, there is one response for each stimulus. In this section, like the experimental results [19], there is no Plateau potential at high frequency (200 Hz) for GPe neurons (Figure 12 c). Based on the results, the frequency of 10 Hz with 3 pulses is the optimal frequency and number of pulses.

3.1.8. Results of ChRwt Four-State Model on RT Network Model

The response of GPe, Gpi, and STN neurons to the ChRwt four-state model and TH output to SMC input in the RT network model with frequencies f=10-200Hz, number of pulses ns=3-40, and pulse width ton=2ms have been evaluated and the results have been reported in Figure 13 (a, b, and c). Also, the correctness of the study has been done with the experimental and computational parameters with the same selection of the parameter's ton, ns, and f, Figure 13. To evaluate the results obtained, the response of GPe neurons to ChRwt four-state stimulation of reference [27] for the frequency 10 Hz and the number of pulses 3 heve been shown in Figure 13d.Comparing the results with GPe neurons shows that at f=10 Hz, there are additional responses for all three GPe, GPi, and STN, and for TH neurons, except for one case which is an additional response, there is one response for each stimulation. For GPe neurons, the response

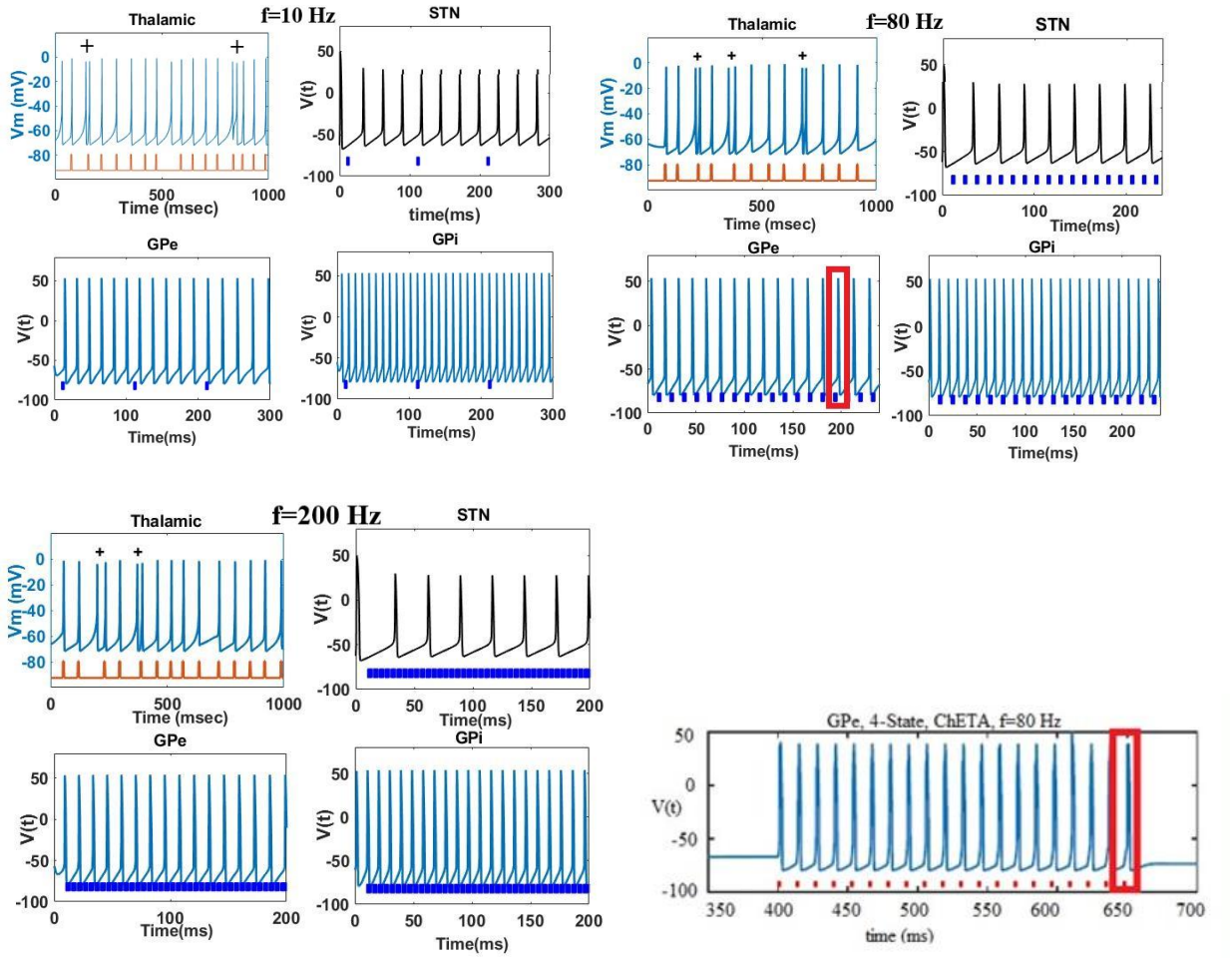

Figure 11. Response of GPe, Gpi, and STN neurons to the ChETA four-state model for RT network model and TH response to SMC (a) f=10 Hz, ns=3, t_{on}=2 ms, (b) f=80Hz, ns=20, t_{on} =2 ms, (c)f=200 Hz, ns=40, t_{on} =2 ms, (d) response of GPe neurons to stimulation for f=80Hz and ns=20 according to ChETA four-state model [19] (rectangular box indicates one response for each stimulation)). (Orange pulses at the output of TH correspond to SMC input pulses, blue pulses at the outputs of GPi, Gpe, and STN are ChETA four-mode stimulation light pulses and red pulses at the output of GPe neurons are for ChETA four-state stimulation light pulses for the experimental and calculation results [19].)

Table 5. Results and responses of BG and RT network model neurons (STN, GPe, GPi, TH) to stimulation of ChETA four-state model with different parameters (A, ns, f, ton)

EI	Response of TH	Response of STN	Response of GPe	Response of GPi	A (mw/mm^2)	ns	t_{on} (ms)	f (Hz)	Optogenetic model
0.18	Missing response	Additional spike	Additional spike	Additional spike	50	3	2	10	four-state ChETA BG
0.12	Missing response	Missing response	Additional spike	Additional spike	50	20	2	80	
0.12	Additional spike	Missing response	One response for each stimulus and lack of Plateau potential [19,27]	Missing response	50	40	2	200	
0.12	Additional spike	Additional spike	Additional spike	Additional spike	50	3	2	10	four-state ChETA RT
0.18	Additional spike	Missing response	One response for each stimulus [19,27]	Additional spike	50	20	2	80	
0.12	Additional spike	Missing response	Missing response and lack of Plateau potential [19]	Missing response	50	40	2	200	

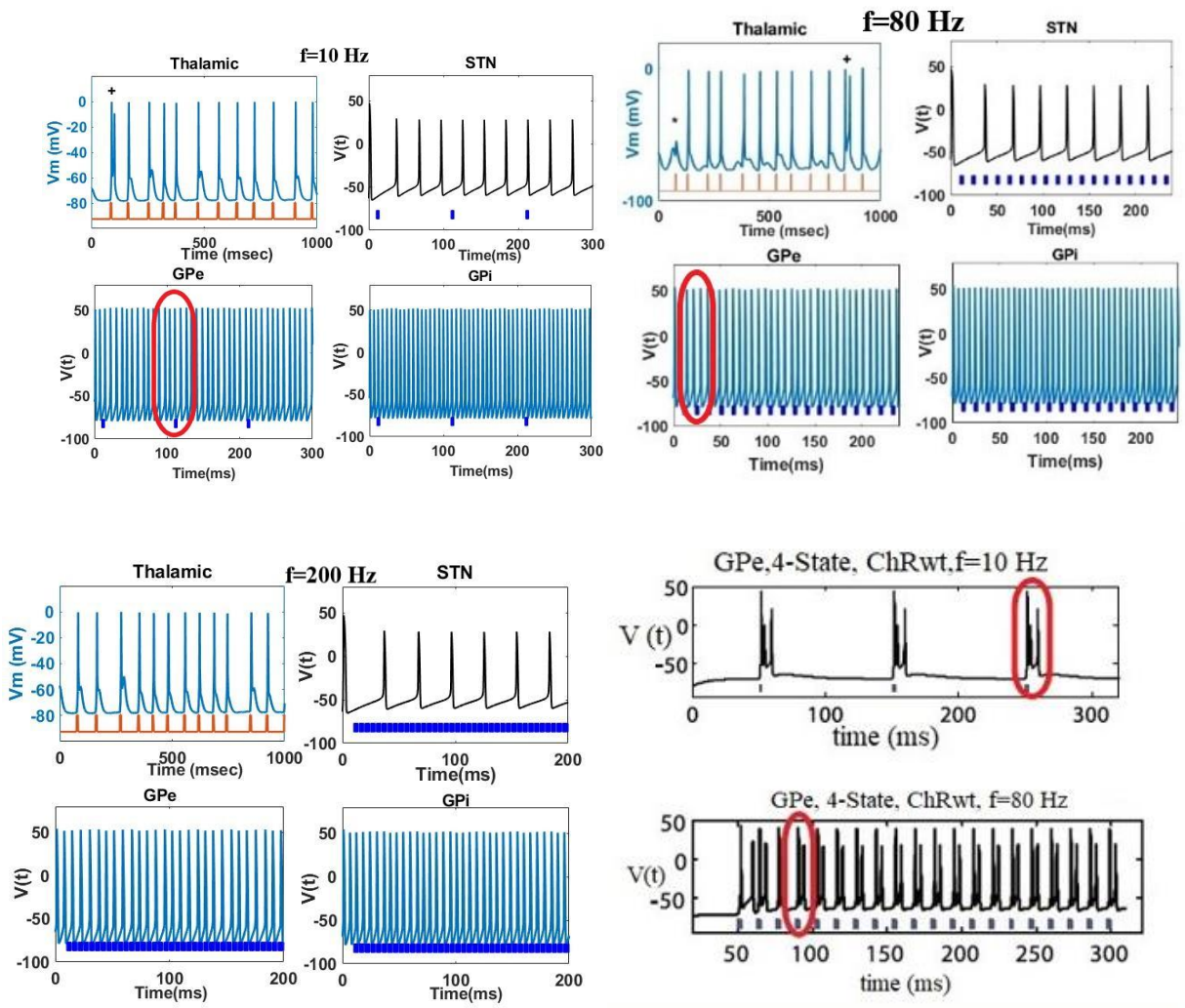

Figure 12. Response of GPe, Gpi, and STN neurons to ChRwt four-state model for BG network model and TH response to SMC (a) f=10 Hz, ns=3, t_{on}=2 ms, (b) f=80 Hz, ns=20, t_{on}= 2 ms, (c) f=200 Hz, ns=40, t_{on}=2 ms (d) response of GPe neurons to stimulation for frequencies f=10,80 Hz and number of pulses ns=3,20 to the ChRwt four-state model [27] (The oval boxes indicate the additional response.) (Orange pulses at TH output are for SMC input pulses, blue pulses at GPi, Gpe, and STN outputs are for the ChRwt four-state stimulation light pulses and red pulses at the output of GPe neurons are for the ChRwt four-state stimulation light pulses for the experimental and calculation results [27].)

is in the form of additional spikes, which is in accordance with the experimental results [19, 27], and for other neurons, the response is high for GPi and TH (with two burst errors). At f=200 Hz, the responses of GPe, Gpi, and STN neurons are less and there is no Plateau potential, and for TH neurons, the number of responses is seen in two cases with an additional response (two errors of bursts). The absence of a Plateau potential at high frequency (200 Hz) for GPe neurons is in accordance with the experimental results [19]. In Table 6, the results and responses of the BG and RT network model neurons (TH, GPe, Gpi, and STN) per stimulation of the ChRwt four-mode model for different parameters (A, ns, f, ton) have been expressed by considering the EI and its compliance with the available experimental and computational results has been checked. Based on the results, the frequency of 10 Hz with the number of pulses 3 and with less EI is the optimal frequency and number of pulses.

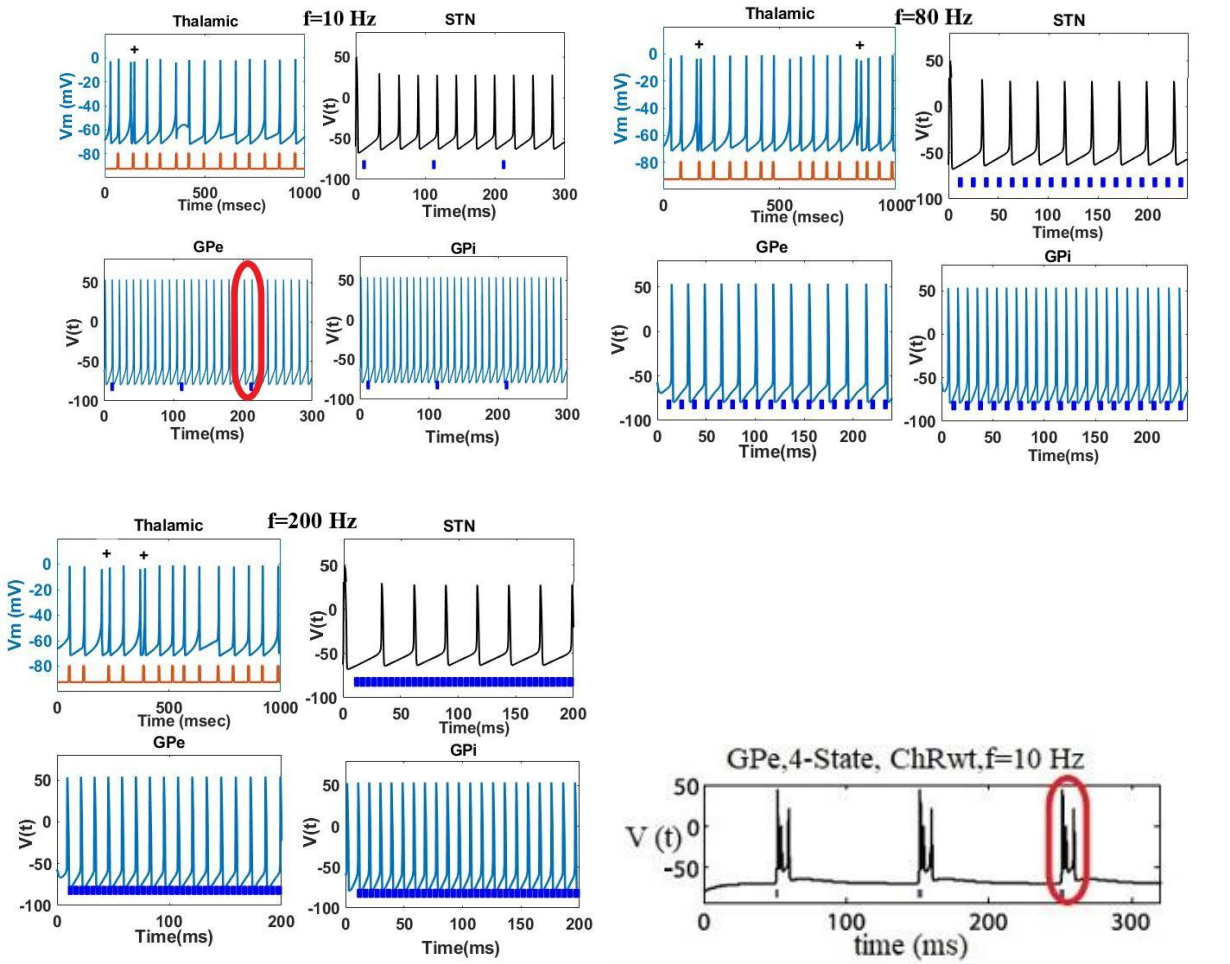

Figure 13. Response of GPe, Gpi, and STN neurons to the ChRwt four-state model for the RT network model and TH response to SMC (a) f=10 Hz, ns=3, t_{on}=2 ms, (b) f=80Hz, ns=20, t_{on}= 2 ms, (c) f=200 Hz, ns=40, t_{on}=2 ms, (d) response of GPe neurons to stimulation for f=10Hz and ns=3 to the ChRwt four-state model [27] (oval box indicates additional response). (Orange pulses at the output of TH are for SMC input pulses, blue pulses at the outputs of GPi, Gpe, and STN are light pulses for the stimulation of the ChRwt four-state model and red pulses at the output of GPe neurons are for light pulses of the ChRwt four-state stimulation for experimental and calculations results [27].)

Table 6. Results and responses of BG and RT network model neurons (STN, GPe, GPi, TH) to stimulation of ChRwt four-state model with different parameters (A, ns, f, ton)

EI	Response of TH	Response of STN	Response of GPe	Response of GPi	A (mw/mm^2)	ns	t_{on} ms	f Hz	Optogenetic model
0.06	Additional spike	Additional spike	Additional spike [19,27]	Additional spike	50	3	2	10	Four-state ChRwt BG
0.12	Additional spike and missing response	Missing response	Additional spike [19,27]	Additional spike	50	20	2	80	
0	One response for each stimulus	Missing response	Missing response and lack of Plateau potential [19]	Missing response	50	40	2	200	
0.06	Additional spike	Additional spike	Additional spike [19,27]	Additional spike	50	3	2	10	Four-state ChRwt RT
0.12	Additional spike	Missing response	Missing response	Additional spike	50	20	2	80	
0.12	Additional spike	Missing response	Missing response and lack of Plateau potential [19]	Missing response	50	40	2	200	

3.2. Prolonged Stimulation Results for the BG and RT Network Models of the ChR2 Optogenetic Model

3.2.1. Prolonged Stimulation Results of Three and Four-State Models for the ChRwt and ChETA for the BG Network Model

Since opsins may lose their effectiveness and function in prolonged stimulation, their response is mostly lost and suppressed, or after a period of time,they do not respond to stimulation at all; in other words, they get reaction fatigue. For this purpose, we have calculated and examined the effects of long stimulation (ns=60) for the three and four-state model for the selected opsins ChRwt and ChETA for the BG network model at a fixed frequency of 20 Hz. Because the results of the three-state model were better, we have reported its results in Figure 14, for the two opsins ChRwt and ChETA for the number of pulses of ns=60 and frequency of f=20Hz. According to the outputs, in the three-state model of the ChRwt for BG, Figure 14a, for STN neurons, the number of responses to stimulation is less and it is accompanied by suppression. For GPe, there is one response for each stimulation, for GPi, the number of responses is more and for TH neurons, there is one response for each stimulation except in three cases (one miss error and two burst errors).

Therefore, in this case, reaction fatigue is seen for STN neurons, but not for other neurons (GPe, GPi, and TH). In ChETA three-state model for BG, Figure14b, there is one response for each stimulation for STN, Gpe, and Gpi cells and we do not have reaction fatigue. For TH neurons, there is one response for each stimulation, except in five cases in the form of additional and missed ones (two burst errors and three miss errors).

3.2.2. Prolonged Stimulation Results of Three and Four-Mode Models for the ChRwt and ChETA for the RT Network Model

In this section, we have also calculated and examined the effects of long stimulation (ns=60) for the three and four-state model for the selected opsins ChRwt and ChETA for the RT network model at a fixed frequency of 20 Hz, and the results of the three-state model have been shown in Figure 15, for the two opsins ChRwt and ChETA, we have provided pulse number of ns=60 and frequency of f=20Hz. In the ChRwt three-state model for the RT network model in Figure 15a, for GPe, GPi, and STN neurons, the number of responses for stimulation is less and suppression, and opsins are fatigued. For TH, there is one response for each stimulation, except in one case an additional response (a burst error) is seen. In ChETA three-state for the RT network model Figure 15b, for GPi, GPe, and STN neurons for each stimulation there is a response and for TH there is also a response for each stimulation except in one case (a burst error). Therefore, reaction fatigue is not seen for neurons.

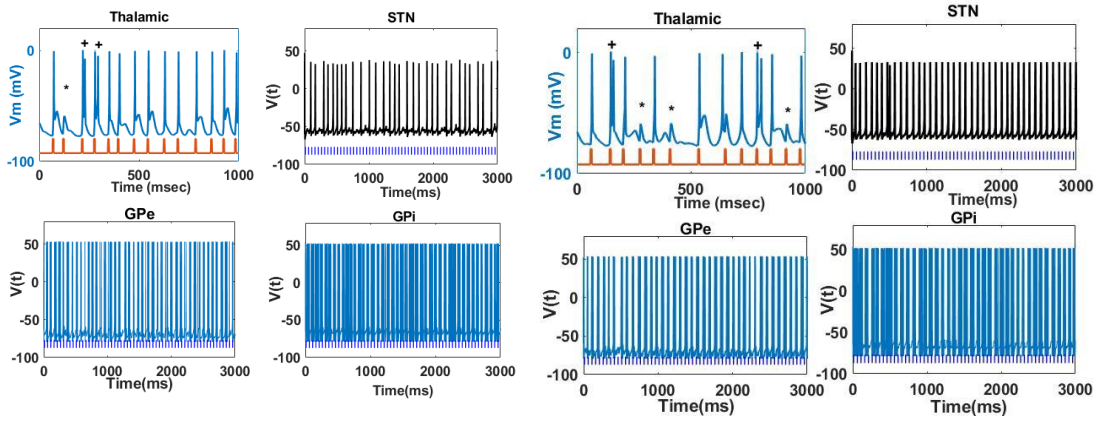

Figure 14. Response of GPe, Gpi, and STN neurons to prolonged stimulation of three-state model for the ChRwt and ChETA for the BG network model and TH response to SMC (a) ChRwt 3-state, f=20 Hz, ns=60, (b) ChETA 3-state state, f=20 Hz, ns=60. (The orange pulses at the TH output are for the SMC input pulses, the blue pulses at the GPi, GPe, and STN outputs are the optical pulses of the three-state stimulation ChRwt and ChETA.)

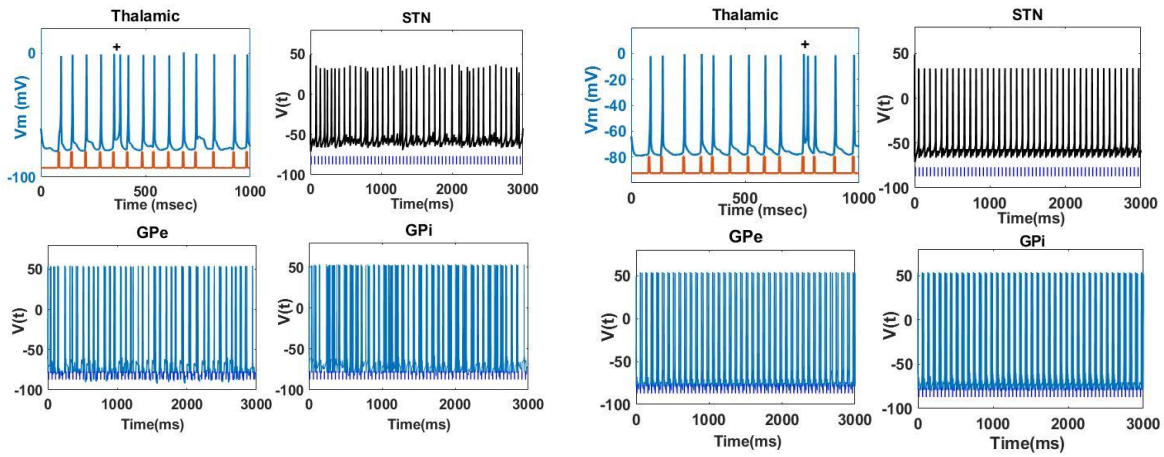

Figure 15. Response of GPe, Gpi, and STN neurons to long stimulation of three-state model for the ChRwt and ChETA for the RT network model and TH response to SMC (a) ChRwt 3-state, f=20Hz, ns=60, (b) ChETA 3-state, f=20Hz, ns=60. (The orange pulses at the TH output are for the SMC input pulses, the blue pulses at the GPi, GPe, and STN outputs are the optical pulses of the three-state stimulation ChRwt and ChETA.)

3.3. Long and Short Stimulation Results for BG and RT Network Models in the NpHR Optogenetic Model

3.3.1. NpHR Results for the BG Network Model

Since brain tissue damage may occur at high frequencies, high intensities of light stimulation, and long pulse widths, in this section we have examined the effects of changing these parameters (f, A, ton) on the response of GPe and GPi neurons and STN model of Parkinsonian network BG. For the optogenetic model of NpHR and the response of TH neurons to SMC, the results have been depicted in Figure 16, for NpHR opsin for frequencies of f=50,100Hz, the number of pulses of ns=30,60, photo stimulation intensities of A=2,50 mw/ mm^2 and pulse width of ton=2,10 ms. Based on the obtained results, it can be said, in Figure 16a.b with increasing ton suppression for STN, GPi, and GPe increased, for TH in Figure 16a, there is one response for each stimulation except in two cases (two bursts) and in Figure 16b, there is one response for each stimulus (no error). In Figure 16c, d with the increase of A, the suppression for STN neurons increased, it did not increase for GPe, and for GPi, it can be seen that the suppression increased to some extent. For TH in Figure 16c, for each stimulation, there is one response except in three cases (two burst errors and one miss), and in Figure 16d, for TH there is one response for each stimulation except in one case (one miss error).

In Figure 16a, d, suppression for GPe and STN has increased with increasing f. Therefore, increasing ton leads to improvement of suppression for GPe, GPi, and STN neurons, increasing A leads to improvement of suppression for STN neurons, and to some extent GPi, and the increase of f has led to the improvement of suppression for GPe and STN neurons by NpHR opsin, and this improvement of suppression of the response of neurons in NpHR by increasing the values of parameters (f, A, ton) leads to no damage to the brain tissue.

3.3.2. NpHR Results for the RT Network Model

In this section, the effects of changing the parameters (f, A, ton) on the response of GPe, GPi, and STN neurons of the RT Parkinson network model for the NpHR optogenetic model and the response of TH neurons to SMC have been investigated and the results have been shown in Figure 17. For NpHR opsin, for frequencies of f=50,100Hz, number of pulses of ns=30,60, intensities of optical stimulation A=2,50 mw/ mm^2 and pulse width of ton=2,10 ms have been shown. Based on the results obtained in Figure 17a, b with increasing ton, the suppression for GPe, GPi, and STN increased, based on Figure 17a, there is a response for TH for each stimulation except in one case (a burst error) and in Figure 17b, there is one

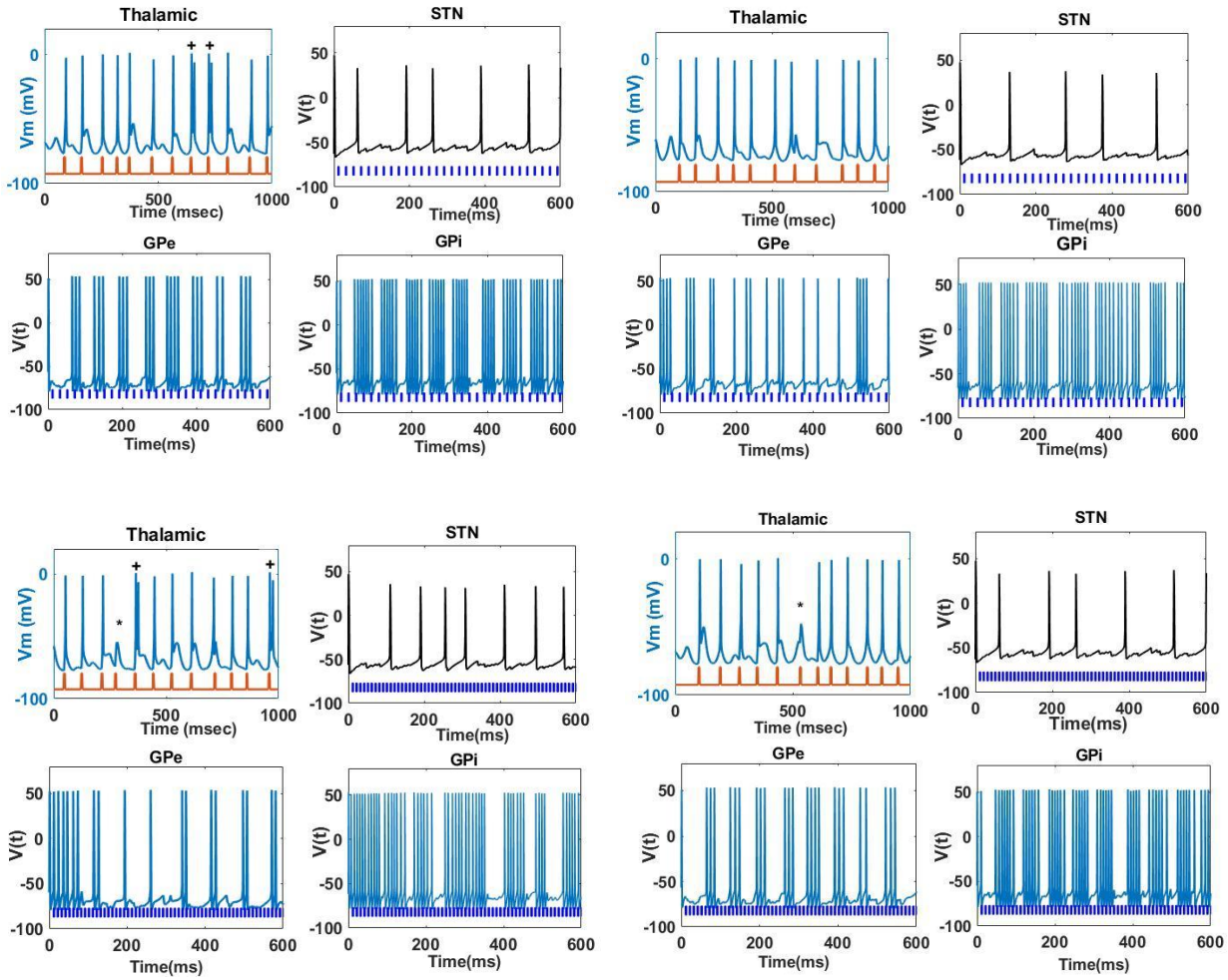

Figure 16. The output of GPe, GPi, and STN neurons of the BG network model for NpHR optogenetics and the response of TH neurons to SMC (a) f=50 Hz, ns=30, A=50 mw/ mm^2, t_{on}=2ms, (b) f=50 Hz, ns=30, A=50 mw/ mm^2, t_{on}=10ms, (c) f=100 Hz, ns=60, A=2 mw/ mm^2, t_{on}=2ms, (d) f=100 Hz, ns=60, A=50 mw/ mm^2, t_{on}=2ms. (The orange pulses in TH output are SMC input pulses, the blue pulses in GPi, GPe, and STN outputs are NpHR stimulation light pulses.)

response for TH for each stimulation except in two cases (a burst error and a miss). In Figure 17c, d with the increase of A, suppression did not increase for STN, but suppression increased for GPe and GPi. For TH in Figure 17c, there is one response for each stimulation except in one case (a burst), and in Figure 17d for TH there is one response (without error) for each stimulation. In Figure 17a, d suppression for GPe, GPi, and STN increased with increasing f. Therefore, increasing ton leads to improved suppression for GPe, GPi, and STN neurons, increasing A leads to improved suppression for GPe and GPi neurons, and increasing f also leads to improved suppression for GPe, GPi, and STN neurons by NpHR opsin, which improves suppression. In the response of neurons with NpHR After increasing the values of the parameters (f, A, t_{on}), it minimizes the possibility of damaging the brain tissue.

3.4. Error index for BG and RT Network Model Evaluation

In this section, we have considered the EI diagram for the ChETA three-state model, ChRwt three-state model, ChETA four-state model, and ChRwt four-state model. for frequencies of f=10,20,80,200Hz to evaluate BG and RT network models. In Figure 18a, the EI diagram has been drawn for the BG network model, based on which the EI range is from 0 to 0.31, and the ChRwt four-state model with two EI=0 at frequencies of 20 and 200 Hz, and also taking the

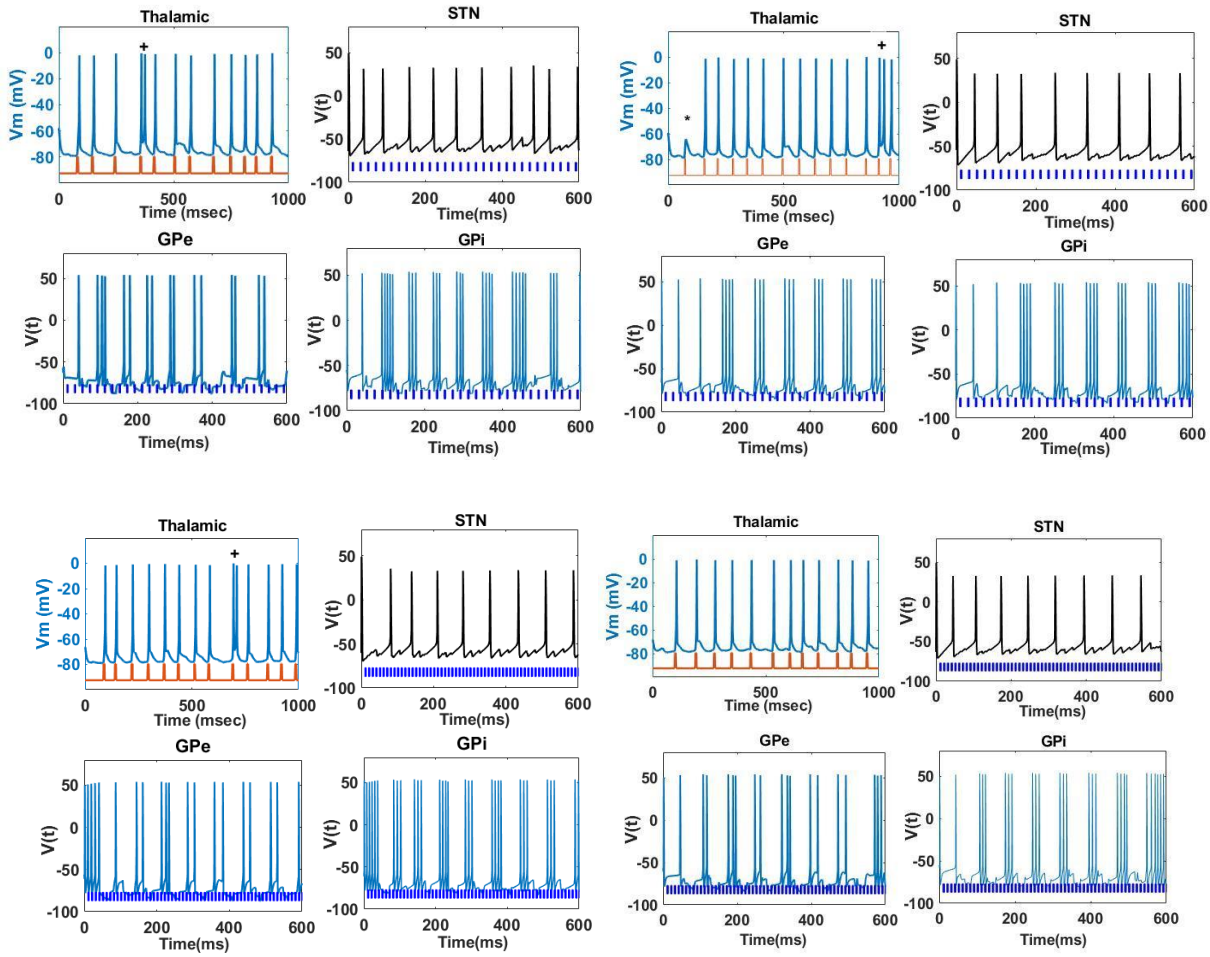

Figure 17. Output of GPe, GPi, and STN neurons of RT network model for NpHR optogenetics and response of TH neurons to SMC (a) f=50 Hz, ns=30, A=50 mw/ mm^2, t_{on}=2ms, (b) f=50 Hz, ns=30, A=50 mw/ mm^2, t_{on}=10ms, (c) f=100 Hz, ns=60, A=2 mw/ mm^2, t_{on}=2ms, (d) f=100Hz, ns=60, A=50 mw/ mm^2, t_{on}=2ms. (The orange pulses at the TH output are for the SMC input pulses, and the blue pulses at the GPi, GPe, and STN outputs are the NpHR stimulation light pulses.)

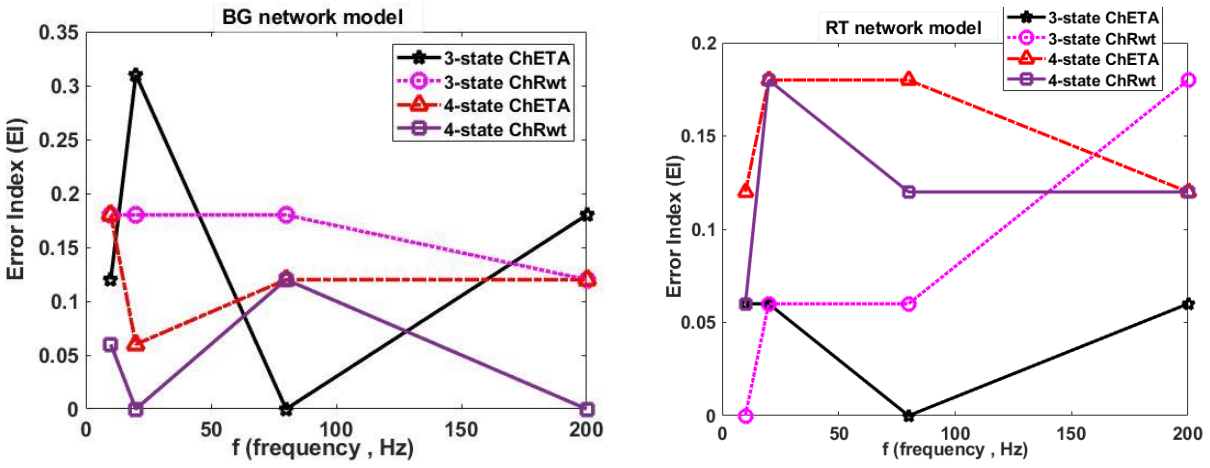

Figure 18. EI diagram for the ChETA three-state model, ChRwt three-state model, ChETA four-state model, and ChRwt four-state model for frequencies of 10, 20, 80, and 200 Hz (a) BG network model, (b) RT network model

lowest range and value for EI (0 to 0.12) is the optimal model. Figure 18b, EI diagram has been drawn for the RT network model, as can be seen, the EI range based on the diagram is 0 to 0.18 and the ChETA three-state model with a case of EI=0 at the frequency of 80 Hz and taking the lowest range for EI (0 to 0.06) is the optimal model.

4. Conclusion

Two complete RT and BG models (including STN, GPe, GPi, and TH neurons) by Rubin-Terman 2004 [32] and Rosa *et al.* 2012 [28] as computational models of the basal ganglia-thalamic network based on the Hodgkin-Huxley model have been introduced. Other simple models that only include parts of basal ganglia neurons (STN-GPe) have been used by Terman *et al.* 2002 [31] to investigate the connections between STN and GPe neurons and their firing patterns (Without studying a specific disease). Shivakeshavan *et al.*, 2017 [29], used a simple model for Parkinson's disease and optogenetic stimulation and only investigated the effect of optogenetic stimulation on STN and GPe neurons in Parkinson's disease. Honghui Zhang *et al.* 2020 [19] also used a simple model for Parkinson's disease and optogenetic stimulation and only reported the response of GPe neurons to optogenetic stimulation in Parkinson's disease.

In this article, to investigate the effect of optogenetic stimulation on Parkinsonian nervous systems, for the first time, we have chosen two complete models of BG and RT (including STN, GPe, GPi, and TH neurons) to simulate the neurons of the basal ganglia nervous system. We have developed it for Parkinson's disease and optogenetic stimulation. Because the models used by other sources (which have studied Parkinson's disease) only include GPe neurons, therefore, for the validation of the used model, we have only used GPe, but after ensuring the correctness of the introduced models, considering that the model used in this paper includes all the neurons of the basal ganglia involved in Parkinson's disease. The effectiveness of other parts including STN, GPi, and TH has been investigated. In previous research references [27-32], limited stimulation parameters have been used, while in this study, a wide range of basic stimulation parameters has been tried to be investigated in order to introduce optimal stimulation conditions.

For this purpose, ChETA, ChRwt, and NpHR opsins and proteins have been examined in three-state and four-state stimulation, and the stimulation conditions include frequency (f), pulse number (ns), pulse width (ton) and stimulation light intensity (A) have been considered. In this paper, we have focused on modeling the pathological conditions of Parkinson's disease and analyzing the effects of three-state and four-state optogenetic stimulation with ChR2 (ChETA, ChRwt) and NpHR opsins. We have used BG and RT network models with GPe, GPi, TH, and STN neurons with different connections. We have also investigated the function of TH neurons and their errors caused by the pathological effects of Parkinson's disease and analyzed the response of both BG and RT network models. To achieve this goal, we have applied different stimulations with different basic parameters (f, ns, A, ton) in both BG and RT network models and introduced optimal conditions (EI=0).

The results obtained from each stage are compared with the existing valid experimental results and the conditions with similar results (one response for each stimulation, suppression of stimulation, and additional response) are introduced. Based on the comparisons, it can be said that the response of GPe neurons is consistent with the experimental results and the response of other neurons is similar to the response of GPe neurons. In optimal conditions, STN neurons provide excitatory input and GPe neurons provide appropriate inhibitory input to GPi neurons, and GPi neurons are able to provide appropriate inhibitory input to TH neurons, and as a result, its function improves and the pathological effects of Parkinson's disease disappear. With prolonged stimulation, the function of opsins may be disrupted and changed, so that most of the responses are inhibitory or there is no response after a period of time.

Therefore, we applied long stimulation (ns=60) to the three- and four-state model with ChRwt and ChETA opsins for BG and RT network models to investigate the effects of prolonged stimulation on the effectiveness of selected opsins. On the other hand, since the application of high frequency, high intensity of optocal stimulation, and long pulse width can lead to damage in the brain tissue, therefore, to investigate this issue, we have investigated the effects of changing these parameters (f, ns, A, ton) on the response of GPe, GPi and STN neurons of the BG and RT Parkinsonian network model for the

optogenetic model with NpHR opsin and the response of TH neurons to SMC.

In the end, we have obtained EI to evaluate the performance of BG and RT for three-state models with ChETA and ChRwt opsins and four-state models with ChETA and ChRwt opsins in different frequency ranges and have introduced the optimal model.

References

1- Samuel Stuart, Lisa Alcock, Brook Galna, Sue Lord, and Lynn Rochester, "The measurement of visual sampling during real-world activity in Parkinson's disease and healthy controls: A structured literature review." *Journal of neuroscience methods*, Vol. 222pp. 175-88, (2014).

2- Elham Samadi, Hessam Ahmadi, and Fereidoun Nowshiravan Rahatabad, "Analysis of Hand Tremor in Parkinson's Disease: Frequency Domain Approach." *Frontiers in Biomedical Technologies*, Vol. 7 (No. 2), pp. 105-11, (2020).

3- Krystal L Parker, Youngcho Kim, Stephanie L Alberico, Eric B Emmons, and Nandakumar S Narayanan, "Optogenetic approaches to evaluate striatal function in animal models of Parkinson disease." *Dialogues in clinical neuroscience*, (2022).

4- R Prashanth and Sumantra Dutta Roy, "Early detection of Parkinson's disease through patient questionnaire and predictive modelling." *International journal of medical informatics*, Vol. 119pp. 75-87, (2018).

5- Vasilis Ntziachristos, "Fluorescence molecular imaging." *Annu. Rev. Biomed. Eng.*, Vol. 8pp. 1-33, (2006).

6- Ralph Weissleder and Vasilis Ntziachristos, "Shedding light onto live molecular targets." *Nature medicine*, Vol. 9 (No. 1), pp. 123-28, (2003).

7- Claudio Vinegoni, Daniel Razansky, Jose-Luiz Figueiredo, Matthias Nahrendorf, Vasilis Ntziachristos, and Ralph Weissleder, "Normalized Born ratio for fluorescence optical projection tomography." *Optics letters*, Vol. 34 (No. 3), pp. 319-21, (2009).

8- Mark G Van Vledder *et al.*, "The effect of steatosis on echogenicity of colorectal liver metastases on intraoperative ultrasonography." *Archives of surgery*, Vol. 145 (No. 7), pp. 661-67, (2010).

9- Osamu Ukimura, Koji Okihara, Kazumi Kamoi, Yoshio Naya, Atsushi Ochiai, and Tsuneharu Miki, "Intraoperative ultrasonography in an era of minimally invasive urology." *International journal of urology*, Vol. 15 (No. 8), pp. 673-80, (2008).

10- Dushyant V Sahani *et al.*, "Intraoperative US in patients undergoing surgery for liver neoplasms: comparison with MR imaging." *Radiology*, Vol. 232 (No. 3), pp. 810-14, (2004).

11- Shabnam Andalibi Miandoab and Robabeh Talebzadeh, "Ultra-sensitive and selective 2D hybrid highly doped semiconductor-graphene biosensor based on SPR and SEIRA effects in the wide range of infrared spectral." *Optical Materials*, Vol. 129p. 112572, (2022).

12- Amir Asadzade and Shabnam Andalibi Miandoab, "Design and simulation of 3D perovskite solar cells based on titanium dioxide nanowires to achieve high-efficiency." *Solar Energy*, Vol. 228pp. 550-61, (2021).

13- Katyani R and Andalibi Miandoab S, "Enhance efficiency in flat and nano roughness surface perovskite solar cells with the use of index near zero materials filter." *Optical and Quantum Electronics.*, Vol. 53 (No. 9), (2021).

14- Silvia Skripenova and Lester J Layfield, "Initial margin status for invasive ductal carcinoma of the breast and subsequent identification of carcinoma in reexcision specimens." *Archives of pathology & laboratory medicine*, Vol. 134 (No. 1), pp. 109-14, (2010).

15- Charlotte Holm, M Mayr, E Höfter, A Becker, UJ Pfeiffer, and W Mühlbauer, "Intraoperative evaluation of skin-flap viability using laser-induced fluorescence of indocyanine green." *British journal of plastic surgery*, Vol. 55 (No. 8), pp. 635-44, (2002).

16- Alexander Erofeev *et al.*, "Light stimulation parameters determine neuron dynamic characteristics." *Applied Sciences*, Vol. 9 (No. 18), p. 3673, (2019).

17- Ruben Schoeters, Thomas Tarnaud, Wout Joseph, Luc Martens, Robrecht Raedt, and Emmeric Tanghe, "Comparison between direct electrical and optogenetic subthalamic nucleus stimulation." in *2018 EMF-Med 1st World Conference on Biomedical Applications of Electromagnetic Fields (EMF-Med)*, (2018): *IEEE*, pp. 1-2.

18- Karl Deisseroth, Guoping Feng, Ania K Majewska, Gero Miesenböck, Alice Ting, and Mark J Schnitzer, "Next-generation optical technologies for illuminating genetically targeted brain circuits." *Journal of Neuroscience*, Vol. 26 (No. 41), pp. 10380-86, (2006).

19- Honghui Zhang, Ying Yu, Zichen Deng, and Qingyun Wang, "Activity pattern analysis of the subthalamopallidal network under ChannelRhodopsin-2 and Halorhodopsin photocurrent control." *Chaos, Solitons & Fractals*, Vol. 138p. 109963, (2020).

20- Allison E Girasole *et al.*, "A subpopulation of striatal neurons mediates levodopa-induced dyskinesia." *Neuron*, Vol. 97 (No. 4), pp. 787-95. e6, (2018).

21- Jan Tønnesen, "Optogenetic cell control in experimental models of neurological disorders." *Behavioural brain research*, Vol. 255pp. 35-43, (2013).

22- Georg Nagel *et al.*, "Channelrhodopsin-1: a light-gated proton channel in green algae." *Science*, Vol. 296 (No. 5577), pp. 2395-98, (2002).

23- Georg Nagel *et al.*, "Channelrhodopsin-2, a directly light-gated cation-selective membrane channel." *Proceedings of the National Academy of Sciences*, Vol. 100 (No. 24), pp. 13940-45, (2003).

24- Caspar Glock, Jatin Nagpal, and Alexander Gottschalk, "Microbial rhodopsin optogenetic tools: application for analyses of synaptic transmission and of neuronal network activity in behavior." *C. elegans: Methods and Applications*, pp. 87-103, (2015).

25- Nir Grossman, Konstantin Nikolic, Christofer Toumazou, and Patrick Degenaar, "Modeling study of the light stimulation of a neuron cell with channelrhodopsin-2 mutants." *IEEE Transactions on Biomedical Engineering*, Vol. 58 (No. 6), pp. 1742-51, (2011).

26- Feng Zhang, Li-Ping Wang, Edward S Boyden, and Karl Deisseroth, "Channelrhodopsin-2 and optical control of excitable cells." *Nature methods*, Vol. 3 (No. 10), pp. 785-92, (2006).

27- Roxana A Stefanescu, RG Shivakeshavan, Pramod P Khargonekar, and Sachin S Talathi, "Computational modeling of channelrhodopsin-2 photocurrent characteristics in relation to neural signaling." *Bulletin of mathematical biology*, Vol. 75pp. 2208-40, (2013).

28- Rosa Q So, Alexander R Kent, and Warren M Grill, "Relative contributions of local cell and passing fiber activation and silencing to changes in thalamic fidelity during deep brain stimulation and lesioning: a computational modeling study." *Journal of computational neuroscience*, Vol. 32 (No. 3), pp. 499-519, (2012).

29- Shivakeshavan Ratnadurai-Giridharan, Chung C Cheung, and Leonid L Rubchinsky, "Effects of electrical and optogenetic deep brain stimulation on synchronized oscillatory activity in parkinsonian basal ganglia." *IEEE Transactions on Neural Systems and Rehabilitation Engineering*, Vol. 25 (No. 11), pp. 2188-95, (2017).

30- Nazlar Ghasemzadeh, Fereidoun Nowshiravan Rahatabad, Siamak Haghipour, Shabnam Andalibi Miandoab, and Keivan Maghooli, "Controlling pathological activity of Parkinson basal ganglia based on excitation and inhibition optogenetic models and monophasic and biphasic electrical stimulations." *Journal of Biosciences*, Vol. 48 (No. 4), p. 40, (2023).

31- Terman, D., et al., Activity patterns in a model for the subthalamopallidal network of the basal ganglia. Journal of Neuroscience, 2002. 22(7): p. 2963-2976.

32- Rubin, J.E. and D. Terman, High frequency stimulation of the subthalamic nucleus eliminates pathological thalamic rhythmicity in a computational model. Journal of computational neuroscience, 2004. 16: p. 211-235.

33- ALFRED Meyer, "The concept of a sensorimotor cortex: its early history, with especial emphasis on two early experimental contributions by W. Bechterew." *Brain: a journal of neurology*, Vol. 101 (No. 4), pp. 673-85, (1978).

34- TJ Torrico and S Munakomi, "Neuroanatomy, Thalamus.[Updated 2021 Jul 31]." *StatPearls [Internet]. Treasure Island (FL): StatPearls Publishing*, Vol. 1(2022).

35- Peter Hegemann, Sabine Ehlenbeck, and Dietrich Gradmann, "Multiple photocycles of channelrhodopsin." *Biophysical journal*, Vol. 89 (No. 6), pp. 3911-18, (2005).

36- Konstantin Nikolic, Patrick Degenaar, and Chris Toumazou, "Modeling and engineering aspects of channelrhodopsin2 system for neural photostimulation." in *2006 International Conference of the IEEE Engineering in Medicine and Biology Society*, (2006): *IEEE*, pp. 1626-29.

37- Jessica A Cardin *et al.*, "Targeted optogenetic stimulation and recording of neurons in vivo using cell-type-specific expression of Channelrhodopsin-2." *Nature protocols*, Vol. 5 (No. 2), pp. 247-54, (2010).

38- Zahra Noraepour, Mohammad Ismail Zibaii, Leila Dargahi, and hamid Latifi, "Modeling and study of Rhodopsin proteins responses to laser light irradiance in ultrafast optogenetic control." (in eng), *Accepted and Presented Articles of OPSI Conferences*, Research Vol. 24 (No. 0), pp. 569-72, (2018).

39- Viviana Gradinaru, Kimberly R Thompson, and Karl Deisseroth, "eNpHR: a Natronomonas halorhodopsin enhanced for optogenetic applications." *Brain cell biology*, Vol. 36pp. 129-39, (2008).

40- Lisa A Gunaydin, Ofer Yizhar, André Berndt, Vikaas S Sohal, Karl Deisseroth, and Peter Hegemann, "Ultrafast optogenetic control." *Nature neuroscience*, Vol. 13 (No. 3), pp. 387-92, (2010).

41- André Berndt *et al.*, "High-efficiency channelrhodopsins for fast neuronal stimulation at low light levels." *Proceedings of the National Academy of Sciences*, Vol. 108 (No. 18), pp. 7595-600, (2011).

42- Xiao-Jing Wang and György Buzsáki, "Gamma oscillation by synaptic inhibition in a hippocampal interneuronal network model." *Journal of Neuroscience*, Vol. 16 (No. 20), pp. 6402-13, (1996).

43- Denggui Fan, Zhihui Wang, and Qingyun Wang, "Optimal control of directional deep brain stimulation in the parkinsonian neuronal network." *Communications in Nonlinear Science and Numerical Simulation*, Vol. 36pp. 219-37, (2016).